

LA²PC 2020 Booklet

LECO Analytical Applications Poster Competition



LECO
EMPOWERING RESULTS

REGISTER

Elemental Analysis Entries

› Macro, Micro?
Comparison of DUMAS analysers
in real conditions

› Trumac CN, a tool to evaluate the
quality of fertilizers humic coating

› IGA Fractional O/N/H
Analyses of Powder Feedstocks
for Additive Manufacturing

› Analysis of Tic-based Alloys Prepared
by Mechanical Alloying and Spark
Plasma Sintering

› Development of a method to analyze
Aluminum alloys powders using the gas
analyzer LECO ONH836

› LECO Boat Crucible as an Aid to
Analysis of Total Organic Carbon (TOC)
Content in Rock Samples

› LECO Spectrum System 2000

› Pretreating lignocellulosic biomass
wastes for the next generation
of solid fuels

› Moisture, Volatiles and Ash in
Biofuels with the TGA801



Separation Science Entries

› VOCs from Wood Fibers Insulation
Materials

› Analytical Pyrolysis Coupled with
Chemometric Methods

› Investigation of Baijiu Aroma Types
and Regional Origin

› Pyro-GC×GC-TOFMS/FID for the study
of organic matter in unconventional
hydrocarbon reservoirs

› Detection of Honey Bee
Disease Through Monitoring Shifts
in Volatile Profiles

› Green and Sustainable Catalysis
Using a Pd Doped Biochar under Mild
Conditions

MACRO, MICRO? COMPARISON OF DUMAS ANALYSERS IN REAL CONDITIONS

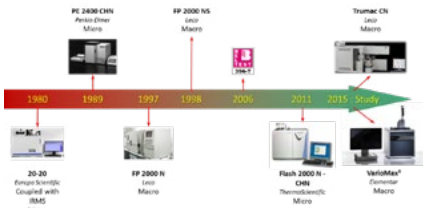
Jean-Michel Romnee | CRAW, Walloon Agricultural Research Centre - Valorization of agricultural products, biomass and wood Unit | Gembloux, Belgium

Charles Ojeimi | ELEMENTAR France | Lyon, France

Alexis Sorokovsky | LECO France | Villepinte, France

Introduction

The comparison of two pieces of equipment allowing the determination of nitrogen and carbon using the Dumas method was carried out as part of an investment designed to supplement the means available in the laboratory. The micro-dumas installed (**Flash 2000[®]**, **ThermoScientific**) do not allow tests above 50 mg, which may limit the technique, particularly for samples with insufficient particle size (heterogeneous sample).



1. History of the Dumas method within the CRAW

The Walloon Agricultural Research Centre is required to determine the organic or total nitrogen content in numerous matrices related to agronomy (soils, plants, agricultural products, human and animal food, fertilisers, fermentation products, etc.). His experience with the Dumas method goes back more than forty years, with the dosage of nitrogen 15, used for tracing fertilisers (Figure 1).

Goal of the study

This study aims to objectify the quality of the two equipment (**TruMac CN[®]**, **LECO – VarioMax^{3®}**, **ELEMENTAR**) likely to meet the specifications and thus choose the equipment that best meets the needs of the laboratory. *Skalar Analytische* preferred to decline the offer to participate in this comparison with the **PrimacsSNC-100[®]**. To evaluate the improvement of the laboratory analysis scheme, the results of the **TruMac CN[®]** and of the **VarioMax^{3®}** were compared with the results obtained using **Flash 2000[®]** (**ThermoScientific**), accredited according to the ISO17025 standard for the determination of the nitrogen content in cereals, cereal products and in food and feed.

Techniques implemented

The determination of the nitrogen content in gaseous effluents resulting from the combustion of samples is based on three principles.

The simplest principle corresponds to determination by gas chromatography (**Flash 2000[®]** – **ThermoScientific**) in which all of the gas effluent is analysed through a catharometer, after chromatographic separation of the various gases to be analysed. In this analysis, no special precautions are taken: the sample is burnt and all of the nitrogen in gaseous form (N₂) is determined. It is therefore possible to relate this quantity to the test sample and to determine a concentration in the sample. However, this implies limiting the number of tests in order to maintain good chromatography.

The second approach is based on the principle of "purge and trap" (**VarioMax^{3®}** – **ELEMENTAR**). In this case, the combustion gases are selectively trapped on molecular sieves and released successively to the catharometer. In this approach too, all the gases emitted pass through the detector.

In the third detection mode, only an aliquot of the gases produced during combustion is analysed (**TruMac CN[®]** – **LECO**). Analysing only an aliquot of gas increases the size of the test portion and reduces the amount of reducing agent per sample. However, the very principle of aliquoting requires collecting a sufficient quantity of gas to be homogenized in the ballast so that the aliquot is representative of all the gases produced.

Experimental comparison protocol

In order to overcome the lack of control of equipment by laboratory staff, the responsibility for analyses has been delegated to the application laboratories (**ELEMENTAR** and **LECO**). The samples were conditioned for direct analyses (grinding and homogenization carried out at Gembloux before sending the samples).

About twenty samples were selected from the stock available to the laboratory. The selected solid samples (18) (cereals, animal feed, protein crops, fodder, soils) were ground on a mill complying with the particle sizes required in the standards used for the determination of the nitrogen content in cereals and in animal feed (ISO 16634-1 and ISO/TS 16634-2). The last two samples are liquid samples (milk and beer).

The samples were then divided into two series of vials of +/- 10g (per sample) and were randomly identified (CRAW-01 to CRAW-40). The CRAW-21 and CRAW-28 (dehydrated alfalfa) samples were limited to approximately 5g per vial, due to quantity available. The CRAW-06 and CRAW-16 samples (extruded soybeans) were repackaged under vacuum in an opaque aluminium bag to protect them from any changes (oxidation, in particular).

EL BIPEA	Nature	Nitrogen content (%) mean ± 2σ	EL BIPEA	Nature	Nitrogen content (%) mean ± 2σ
2014.06	Straw	0,566 ± 0,080	2014.05	Dehydrated alfalfa	2,904 ± 0,146
2014.02	Dactyl hay	1,040 ± 0,080	2014.04	Colza	3,024 ± 0,096
2014.10	Corn	1,184 ± 0,064	2014.06	Pea	3,072 ± 0,096
2014.04	Alveograph flour	1,468 ± 0,040	2014.02	Feed for turkey	3,856 ± 0,112
2014.09	Alveograph flour	1,613 ± 0,046	2014.05	Dog feed	4,736 ± 0,144
2014.05	Alveograph flour	1,797 ± 0,051	2014.12	Extruded soya beans	5,856 ± 0,176
2014.01	Alveograph flour	2,069 ± 0,058	2014.04	N corrector with urea	6,976 ± 0,208
2014.11	Feed for laying hens	2,640 ± 0,080	2014.11	Fish meal	11,024 ± 0,336
	Milk	0,550		Soil 01	0,060
	Beer	1,120		Soil 02	1,180

Table 1: List of samples studied in the context of the comparison study

The BIPEA results for alveograph flours are expressed at 100% dry matter. To avoid determining the dry matter in the Application labs (the determination of the dry matter on flour requires a special oven that is only found in the laboratories concerned with the analyses of cereals), the nitrogen contents have been reduced to an expression on fresh matter, like the other samples.

These samples cover a particularly wide range of nitrogen contents and have different natures (cereals, animal feed, protein crops, food supplement, soil, fodder, etc.). For BIPEA samples, the nitrogen content, the result of an inter-laboratory test (together with its standard deviation) is considered as the target value to be reached. For the four samples from CRAW (milk, beer and soils), the reference value was calculated by averaging the 8 measurements for the sample (double blind * two days * two laboratories). The series of forty samples was analysed twice (two different days) under reproducibility conditions.

Results

As part of the study carried out, not all the parameters used for the validation of analytical methods will be studied. Only the following parameters were analysed: trueness, precision (repeatability, short-term repeatability and reproducibility) and robustness, with reference to the standards relating to the different matrices analysed: **ISO 16634-1:2009** (Food products – Oilseeds and animal feeding stuffs) – **ISO 16634-2:2016** (Food products – Cereals, pulses and milled cereal products) – **ISO 14891:2002** (Milk and milk products) – **NBN EN 16148 (2012)** (Sludge, treated bio-waste and soil) – **EBC 9.9.2. (1999)** (Total Nitrogen in Beer: Dumas Combustion Method).

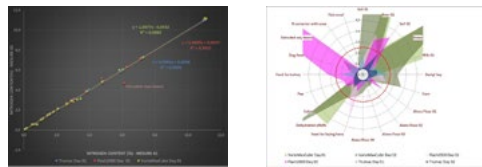
Repeatability

The repeatability was evaluated from the doubles (results obtained in double blind) on days 01 and 02. The difference between double was compared for each sample, with the corresponding standard (when it was available) and the relation between both measurements was characterized for both days and for all data.

	Flash 2000 [®]	TruMac CN [®]	VarioMax ^{3®}
	Respect for limits	16 / 17	14 / 17
Day 01	Regression (M1,M2)	M2 = 1,005 M1 – 0,0257	M2 = 1,0047 M1 – 0,0067
	R ²	0,9997	0,9999
Day 02	Respect for limits	16 / 17	15 / 17
	Regression (M1,M2)	M2 = 0,9728 M1 + 0,0332	M2 = 1,0003 M1 – 4E-5
Global	R ²	0,9848	0,9988
	Respect for limits	32 / 34	34 / 34
Global	Regression (M1,M2)	M2 = 0,9889 M1 + 0,0037	M2 = 0,9981 M1 + 0,0056
	R ²	0,9922	0,9999

Table 2: Summary of the "Repeatability" comparison between the three devices

Table 2 presents a summary of the comparison for the parameter "Repeatability". Of the three devices compared, only the **TruMac CN[®]** gave daily results that met all repeatability standards. The R² obtained for the **TruMac CN[®]** relations are higher, without being different from the others. The **VarioMax^{3®}** encountered problems when determining the nitrogen content in three different samples (Milk, Dehydrated alfalfa and Colza). For the **Flash 2000[®]**, the problems were at the level of feed for poultry (hens and turkeys).



2. Repeatability: example of Day 01 and coefficient of variation measured for each pair of samples

The coefficient of variation, calculated for each pair of results over the two days, completes the information on repeatability. Thus, only the **TruMac CN[®]**, for all of its results (Figure 2), respects an arbitrary limit of 2% for the coefficient of variation.

The results presented in Figure 1 clearly show that the three equipment are particularly well suited to determining the protein content in cereals since the variation coefficients are much less than one percent for this type of matrix. They deteriorate once the matrix becomes more complex and becomes more difficult to grind (fatty food, for example). This matrix-test socket combination can lead to very high coefficients of variation for **Flash 2000[®]**.

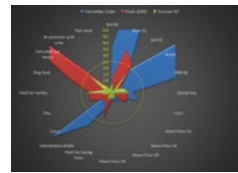
Intermediate precision

Intermediate precision is evaluated by comparing the results obtained for the same sample on the two days of analysis. The first approach lies in the relation between these two values (linear regression) and the second in the comparison between the difference measured for a double and the reproducibility limits defined in the standards (function of the matrix) (Table 3).

	Flash 2000 [®]	TruMac CN [®]	VarioMax ^{3®}
Respect limits	34 / 34	33 / 34	33 / 34
Equation D _i = f(D _i)	D _i = 0,98 D _i + 0,018	D _i = 0,9993 D _i + 0,0011	D _i = 1,0005 D _i – 0,0065
R ²	0,9905	0,9994	0,9992

Table 3: Summary of the parameter "Intermediate precision"

A complementary approach to reproducibility is based on the calculation of the coefficients of variation calculated not on the duplicates but on the samples, or by integrating the four measurements (doubles from day 01 and doubles from day 02). Figure 3 shows that the **TruMac CN[®]** exhibits coefficients of variation of less than 2.5% for all samples. The results obtained for straw and rapeseed lead to CVs (%) greater than 5% for the **VarioMax^{3®}**.



3. Intermediate precision: Coefficients of variation calculated per sample (2 days * 2 measurements)

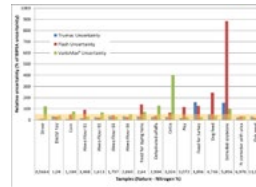
Accuracy

For each of the samples from the BIPEA, the laboratory has a reference value with an uncertainty. These two elements were incorporated into the trueness assessment. Table 4 provides the regression equations calculated on the results obtained for each of the techniques.

	Flash 2000 [®]	TruMac CN [®]	VarioMax ^{3®}
Lab = 1,0101 BIPEA – 0,103	Lab = 1,0082 BIPEA + 0,003	Lab = 1,0199 BIPEA – 0,0414	
R ² = 0,9993	R ² = 0,9991	R ² = 0,9989	

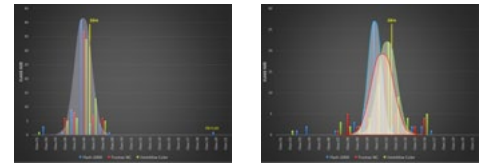
Table 4: Summary of the parameter "Intermediate precision"

The three devices monitored show an excellent relationship between the values obtained in the laboratory and the BIPEA reference values. These relationships can be completed by observing the relative uncertainties (Lab uncertainty related to the BIPEA uncertainty, in %, Figure 4).



4. Relative uncertainty (Lab uncertainty referred to the BIPEA uncertainty, expressed in %)

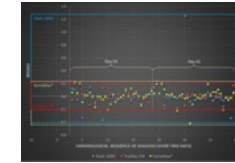
Figure 4 shows that, although the regressions are excellent for the three series of samples, the relative uncertainties are greater than 100% for 7 samples for the **Flash 2000[®]** and for the **VarioMax^{3®}**, while the overshoot is only found for 2 samples for the **TruMac CN[®]**. The accuracy of the results obtained for each piece of equipment was supplemented by an evaluation of the distribution of residuals. These are defined as the difference between the Lab value, estimated from the BIPEA, and the measured Lab value. The relationship defined between the lab values and the BIPEA values makes it possible to calculate the estimated Lab value. The distribution of the residuals must have the appearance of a Gaussian curve, centred at zero, which is found in Figure 5, for the three equipment studied.



5. Distribution of residuals (left : 21 classes with amplitude of 0.09, from -0.5 – right : 21 classes with amplitude of 0.045, from -0.5, with elimination of the "Outlier" value)

All three distributions appear centred on the same maximum when the extreme value (**Flash 2000[®]**) is taken into account. The average of the residuals is equal to 0,0001 (**TruMac CN[®]** and **VarioMax^{3®}**) and -0,0001 (**Flash 2000[®]**). Dividing the class amplitude by two reveals some differences for the class with the maximum number of students and for the spread of the distribution (width at the base).

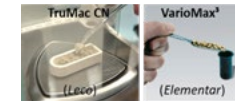
The chronological distribution of the residuals over the two days that the analyses were performed (Figure 6) effectively shows that the residuals range of the **TruMac CN[®]** is well centred on zero and has the lowest amplitude. Both the **Flash 2000[®]** and the **VarioMax^{3®}** would have the same distribution if there were only a few samples that were largely out of range. The central area of the samples clearly shows the accuracy of the flour analysis, with very low residues. The amplitude of the residues increases with the type of sample (fat, heterogeneous grinding).



6. Chronological distribution of residuals

Implementation of the analysis

The practicality of the analysis was also assessed during the study. Weighing and cup filling, which is simple for one or two samples, proved to be less cumbersome for the **TruMac CN[®]** than for the **VarioMax^{3®}**. This is because the filling of the basket is done in a more natural motion for the **TruMac CN[®]** (Figure 7). The preparation of the nickel foils for the **Flash 2000[®]** was not taken into account, even though this step is particularly "time-consuming".



7. Ease of filling the buckets

Conclusion

The objective of this study was to compare two macro-dumas equipment (**TruMac CN[®]**, **LECO – VarioMax^{3®}**, **ELEMENTAR**) allowing the determination of the nitrogen content in different agricultural and agro-food matrices according to the Dumas method, using test samples of the order of 500 mg, in order to complete the micro-dumas equipment available in the laboratory.

The study involved the analysis of 40 samples (20 in double blind) repeated two days in a row. Sixteen samples came from the BIPEA sample stock (for which the laboratory has a target value and uncertainty), to which were added two soils, one milk and one beer. The application laboratories of the two firms concerned carried out the analyses and sent the results to CRAW, which analysed the data.

The study showed that, despite being ISO17025 accredited, the **Flash 2000[®]** (Interscience, micro-dumas) showed greater variability in the results than the two pieces of equipment studied, which can easily be explained by the reduced size of the test sample (maximum 50 mg compared to 500 mg).

The differences between **TruMac CN[®]** and **VarioMax^{3®}** were particularly marked for the more specific samples (high fat content, difficult to grind, heterogeneous matrix). The performance of **TruMac CN[®]** was better for these samples, whereas for easy to prepare samples (e.g. flour) both machines gave equivalent results.

While the regressions obtained between Lab and BIPEA values are excellent, the relative uncertainties are better for the **TruMac CN[®]** for which only two samples have a relative uncertainty greater than 100% (BIPEA Uncertainty) while seven samples exceed this threshold for the **Flash 2000[®]** and **VarioMax^{3®}**.

TRUMAC CN, A TOOL TO EVALUATE THE QUALITY OF FERTILIZERS HUMIC COATING

Jean-Michel Romnee | CRAW, Walloon Agricultural Research Centre – Valorization of agricultural products, biomass and wood Unit | Gembloux, Belgium



Introduction

The term "humic substance" is a generic name given to a large number of amorphous and colloidal organic polymers formed during the decomposition of the organic matters. The humic substances can be divided into three principal fractions based on their solubility in the acids and/or the bases. The soluble fraction in the acids and the bases is called acid fulvic. It has the weakest molecular weight. That which is soluble in the bases but precipitates in the acids is the humic acid, and that which is insoluble in the acids and the bases is humin.

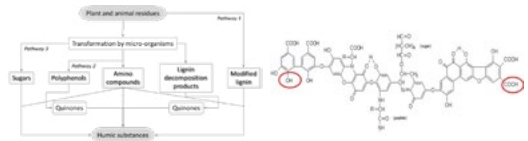


Figure 1: Pathways for humic substances formation [after Stevenson, 1994]
Figure 2: Humic substance

Humic substances are of interest in agronomy through their stimulating effect on plant growth. However, the different possible formation pathways imply heterogeneity in their composition, making their characterization difficult.

Currently, humic substances are mainly extracted from Leonardite, but they represent a significant way of recovering organic waste, thus reducing the inputs necessary for agriculture, while being part of a sustainable waste recycling policy.

The protocols for characterization of humic substances can be divided into two groups: destructive protocols and non-destructive protocols. The destructive protocols are based on hydrolyses of the organic material and successive extractions under different pH conditions. The analysis will therefore consist in identifying and assaying structural units (for monomers) serving as a basis for the macromolecules constituting humic substances, identifying the functional groups of these structural units and carrying out an elemental assay (C, H, N and O). The methods implemented in these different assays are chemistry or separation and conventional identification methods (gas chromatography, [ultra] high pressure liquid chromatography, mass spectrometry, etc.). However, they do not provide information on the actual arrangement of structural units in macro-molecules. The non-destructive protocols are based on physical methods which do not necessarily require the extraction of the compounds to give a characterization (UV spectroscopy [ultraviolet], IR spectroscopy [infra-red], NMR spectroscopy [nuclear magnetic resonance]). However, they often require calibration for quantitative use, which requires strict monitoring of a destructive protocol.

Goal of the study

To avoid long and tedious analytical techniques, we used the Trumac CN to assess the humic substance content of coated fertilizers and to assess the quality of the coating.

Having available a series of eight "humic substances" substrates (Sub-01 to Sub-08) and three mineral fertilizers in the form of granules (SUPP-01 to SUPP-03), we prepared four coated fertilizers (ENG-01 to Eng 4) on which various analyses were carried out to check the carbon contents on the coated fertilizers, both in quantity and quality of coating.

To make the coated fertilizers, two aqueous solutions mixing several of the humic substances were prepared and sprayed on the mineral fertilizers, simultaneously with a supply of additional humic substances, used as glue, in a mixer. All these steps were done in quantitative ways, thus making it possible to measure the carbon and nitrogen content at each step (on raw materials and products) and to check the quality of the preparation work.

ENG-02 and ENG-03 fertilizers are prepared from the same carrier fertilizer (SUPP-03).

Analyses carried out

The determination of the C and N content was carried out on the raw materials, on the solutions and on the coated fertilizers (as is, grinded and granulated form, by granule). We have sought to maintain test doses in the order of 500 mg. Humic substances and aqueous solutions were analysed in duplicate and coated fertilizers were analysed in triplicate.

Results

Raw material analysis

Table 1 shows the percentages of carbon and nitrogen measured on the raw materials: humic substances (SUB) – coating solutions (SO) – mineral fertilizers (SUPP). The nitrogen contents are generally very low for humic substances (from 0.01% to 3.19%), the coating solutions having nitrogen contents of less than 1%. For carbon, the contents of humic substances are much more variable (from 0.68% to more than 35%). Both solutions contain around 15% carbon.

Samples	Mean Nitrogen (%)	Standard deviation	RSD %	Mean Carbon (%)	Standard deviation	RSD %
SUB-01	0.01	0.002	15.01	8.72	0.208	2.38
SUB-02	0.03	0.011	41.49	0.68	0.009	1.31
SUB-03	0.02	0.009	49.65	7.61	0.050	0.65
SUB-04	0.22	0.0004	0.20	3.67	0.004	0.11
SUB-06	3.19	0.005	0.14	11.46	0.421	3.67
SUB-07	0.69	0.003	0.47	36.34	0.028	0.08
SOL-01	0.92	0.001	0.07	16.42	0.066	0.40
SOL-02	0.28	0.003	0.99	14.93	0.090	0.60
SUPP-01	24.39	0.592	2.43	3.12	0.109	3.49
SUPP-02	17.70	0.006	0.04	0.78	0.010	1.24
SUPP-03	45.96	0.153	0.33	20.74	0.066	0.32

Table 1: Determination of the C (%) and N (%) content on raw materials: humic substances (SUB) – coating solutions (SO) – mineral fertilizers support (SUPP)

Based on the coated fertilizer preparation sheets, it was possible to calculate a theoretical carbon and nitrogen content, and to compare these contents with the contents measured directly on the fertilizer granules (Table 2). Except for the ENG-04 fertilizer which has a very low carbon content (around 2%), the average contents obtained during the analysis of the coated fertilizer granules are similar (from 101.5% to 104.6%) values obtained by calculation. The variation coefficients are less than 4%, except for carbon of the ENG-04 fertilizer (5.18%).

	ENG-01 SUPP-01	ENG-02 SUPP-03	ENG-03 SUPP-03	ENG-04 SUPP-02
Mean _{calc}	21.69	3.81	40.89	19.48
SD _{calc}	0.59	0.15	0.15	0.11
RSD %	2.73	3.93	0.37	0.54
Mean _{analy}	22.69	3.90	41.51	19.87
SD _{analy}	0.09	0.13	0.44	0.14
RSD %	0.41	3.28	1.05	0.69
Mean _{analy} versus Mean _{calc} (%)	104.6	102.3	101.6	102.1

Table 2: Determination of the C (%) and N (%) content on coated fertilizers

For the four coated fertilizers, the analyses carried out show that the granule preparation process meets the expected levels. The lower carbon contents, however, show more variations (ENG-04).

Influence of grinding

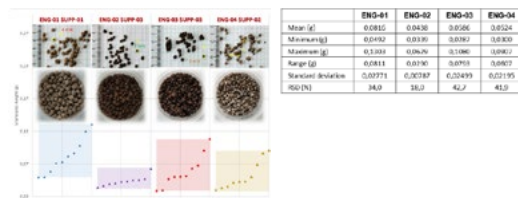
Table 3 compares the measured carbon and nitrogen contents of coated fertilizers, in the form of granules, as used and in the form of ground material. These results illustrate the benefit of grinding, particularly on samples with a low carbon content.

	Nitrogen (%)		Carbon (%)	
	Granulated	Grinded	Granulated	Grinded
Mean	15.87	15.80	1.70	1.85
SD	0.03	0.02	0.14	0.01
RSD %	0.19	0.10	8.08	0.65

Table 3: Determination of the C (%) and N (%) content on coated granulated and ground fertilizers (ENG-04 SUPP-02)

Coating quality

To assess the quality of the coating, for each fertilizer, 96 granules were randomly placed in a microplate. Among these 96 granules, 10 were taken at random and analysed individually (N % and C %).



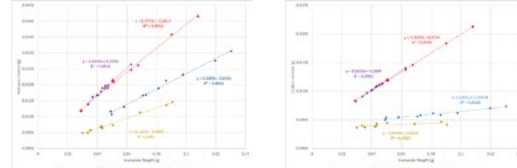
3. Coated fertilizers obtained: pellet size distribution

Figure 3 summarizes the distribution of the forty granules analysed. Although based on the same medium, ENG-02 and ENG-03 fertilizers have very different distributions. The essential difference between the two fertilizers is the use of two humic substances (SUB-02 and SUB-03) as a coating, in addition to the solution, for ENG-03 while only one (SUB-03) is used for ENG-02.

10 granulates of each fertilizer	ENG-01 SUPP-01	ENG-02 SUPP-03	ENG-03 SUPP-03	ENG-04 SUPP-02
Mean	23.22	7.83	42.26	24.92
Standard deviation	0.817	1.777	1.061	1.238
RSD (%)	3.52	22.71	2.51	4.97

Table 4: Determination of the C (%) and N (%) content on individual granulate of coated fertilizers – globalisation of results

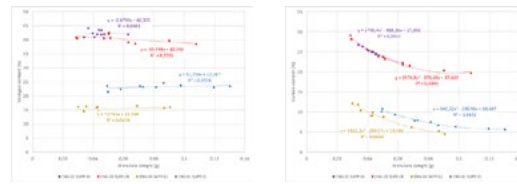
Regarding the origin of the two dosed elements, for the coated fertilizers, almost all of the nitrogen (> 99.9%) is found in the support fertilizer, which leads to a direct relationship between the mass of the granulated and the amount of nitrogen present. For carbon, SUPP-03 contains more than 95% of the carbon, while this percentage drops to around 75% for SUPP-01 and only 35% for SUPP-02.



4. Coated fertilizers – relationship between the amount of element present and the mass of the fertilizer granule

For coated fertilizers using this support (ENG-04), the carbon content, although very low, is much less dependent on the mass of the support granule.

Figure 4 clearly shows that the quantity of nitrogen is directly linked to the coated fertilizer test sample and that the angular coefficient of the regression line practically corresponds to the percentage of nitrogen present.



5. Coated fertilizers – relationship between the percentage of element and the mass of the granule analysed

This is because the nitrogen comes exclusively from the support. For carbon, for ENG-02 and ENG-03, for which more than 95% of the carbon comes from the support, the same type of direct relationship between quantity of carbon and mass of the sample is observed, although the angular coefficient of the right no longer corresponds to the percentage of carbon. As the fraction of carbon coming from the support decreases, the amount of carbon is less and less dependent on the mass of the sample, which can be explained by the low amount of coating placed on the fertilizer grains.

For nitrogen, the percentage therefore remains a constant, regardless of the mass of the sample taken (Figure 5). For carbon, this percentage decreases according to a quadratic function of the sample mass, the coefficient R² being significantly improved between linear regression and polynomial regression (Table 5).

	C _{content} = a.GW _g + b	C _{content} = a'.GW _g ² + b'.GW _g + c'
ENG-01 SUPP-01	R ² = 0.8791	0.9841
ENG-02 SUPP-03	0.9601	0.9912
ENG-03 SUPP-03	0.8145	0.9841
ENG-04 SUPP-02	0.9388	0.9689

Table 5: Evolution of R² between linear regression and polynomial regression

Using the masses of the individual fertilizer granules, as well as their C and N contents, the overall percentage of each element was calculated for the ten grains and compared to the percentage obtained on the ground coated fertilizer granules (Table 6).

	ENG-01	ENG-02	ENG-03	ENG-04
Powder	22.69	3.90	41.51	19.87
Globalisation of the 10 individual measurements on fertilizer granules	23.32	7.32	42.26	24.72

Table 6: Comparison of the percentages of N and C, calculated globally for the 10 coated fertilizer granules, with the percentages obtained on the coated fertilizer powder

While the match is excellent for the N contents, the more the C percentage decreases, the more it is overestimated for the individual determinations. Analysis of the raw data, and more particularly the surfaces obtained for carbon, highlighted the importance of very precise blank calibration. In fact, the areas obtained for the carbon on the individual granules with a low C content are very small (from 350 AU to 2,000 AU) compared to the areas obtained for the carbon contained in the blanco (200 – 300 AU). A very small variation in the C content in the gas analysed will therefore have a strong impact on the percentage since the test sample is very low (of the order of a few tens of milligrams).

Blank calibration was introduced systematically at the start of the analysis series, which made it possible to increase the difference between the areas measured for blanco and the low carbon samples (based on individual granules). When analysing a test portion of the order of 500 mg, the problem does not arise because the quantity of carbon to be measured is high enough so that the corresponding surface is no longer disturbed by variations in the blanco.

	N content (%)		C content (%)		C/N ratio	
	March 29, 2018	October 29, 2018	March 28, 2018	October 29, 2018	March 29, 2018	October 29, 2018
ENG-01	22.69	23.56	103.8	3.90	3.00	76.9
ENG-02	41.51	40.47	97.5	19.87	17.70	89.1
ENG-03	40.78	39.56	97.0	19.60	17.79	90.8
ENG-04	15.80	15.53	97.8	1.70	1.15	67.6
ENG-04 (grinded)	15.87	15.62	98.9	1.85	1.18	63.6

Table 7: Evolution of the C and N content over a period of seven months – Variation of the C/N ratio over the same period

The results obtained on the samples (coated granules) after seven months of storage in the laboratory (in the dark and away from humidity) show that the samples of fertilizers coated with humic substances can change (Table 7): if N content is relatively stable, C content, expressed in %, decreased slightly after this storage, as did the C/N ratio, parameter used in fertilization.

This decrease in carbon content could be explained by the evolution of humic substances used as coating. In fact, assuming that carbon is representative of humic substances, the ENG-02 and ENG-03 samples exhibit C losses of around 10% (for 5% of the C present in the coating). ENG-04 presents C losses of the order of 32.5% (for 65% of the C present in the coating). ENG-01 is intermediate in terms of C present in the coating (25%) and its losses in C are less than those of ENG-04 since they amount to 24%. For ENG-04 (grinded), it should be noted that it is the crushed material that was kept. The losses are greater (36.5%) than those observed for ENG-04 in granular form. The accessibility of the coating materials seems important to explain these losses. It would therefore be useful to study the evolution of humic substances during storage in order to allow manufacturers to provide a product that meets the requirements and farmers to use the right dose of fertilizer.

Conclusion

This study sought to assess the potential of Trumac CN as a tool for monitoring the quality of the coating of humic substances in coated mineral fertilizers.

The results obtained showed that it was necessary to assess the quality of the coating of mineral fertilizers using humic substances. This assessment was based on the carbon content measured in coated fertilizers and in humic substances used for the coating. Knowing the formulation of the various components of the coated fertilizer, the quality of the preparation of the granules was validated by monitoring the dosage of nitrogen, present mainly in the granules of carrier fertilizer, and carbon. The percentage of carbon expected depending on the humic coating was verified on the final fertilizers. The results obtained show that the coating technique works very well since the C and N contents, measured on the coated fertilizers, correspond practically to 100% to the expected contents.

Analysis of the individual granules demonstrated the importance of the blanco calibration for samples with low C content. When analysing a 500 mg test portion, this importance became relative: in fact, the carbon contents obtained on the coated fertilizers in the form of granules or ground corresponded to the contents calculated based on the formulations.

The manufacturer, a supplier of mineral fertilizers coated with humic substances, therefore has a rapid analyser to assess the initial quality of his product and above all, to monitor the development of this product over time. However, it is essential to work with an analyser that allows sufficiently high samples to be taken to analyse fertilizers with a very low C content, thus allowing the detection of small variations, potential signs of deterioration of the product. Indeed, the conservation of coated fertilizers for 7 months has led to the identification of carbon losses linked to the accessibility of humic matter.

Monitoring the individual quality of the coating turns out to be more difficult because the test samples (individual fertilizer granules) are very low. It would be interesting to master the determination of carbon on these granules because the study of the thickness of the coating layer could be a "quality" indicator. The modelling of the thickness calculation, however, requires knowledge of the density of the carrier fertilizer and the material used as coating, as well as the assimilation of coated granules into spheres. With the knowledge of these parameters, a model could be developed.

IGA FRACTIONAL O/N/H ANALYSES OF POWDER FEEDSTOCKS FOR ADDITIVE MANUFACTURING



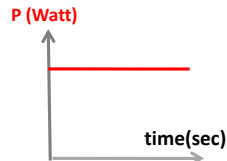
Eurofins EAG Laboratories, Boris ALBOUY, Jérémy BEROT-LARTIGUE, Nicole CUQ (Toulouse / France), Xinwei WANG (NY Syracuse / USA)

Introduction

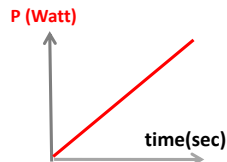
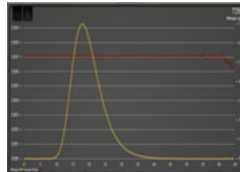
Additive manufacturing calls for powder feedstock of metals, alloys and ceramics, with particle size typically in 100s nm–10 μ m range. This leads to orders-of-magnitude increase in surface area from the bulk materials. Driven by the increase in surface free energy (i.e., thermodynamic favorable) and the decrease in diffusion length (i.e., kinetic favorable), the surface chemistry of powders becomes equally important to, if not greater than, the bulk chemistry. Of particular interest is to understand and control the O, N and H chemistries of powders, which are prone to change depending on the material type, the powder manufacturing technique, working atmosphere, packaging/handling, etc.

Interstitial Gas Analyses (IGA) is the standard method to determine bulk content of O, N and H in inorganic materials, such as metals, alloys and ceramics, via carbo-reductive inert gas fusion, or hot extraction-induced dehydrogenation, followed by infrared or thermal conductivity detection. Taking advantage of the temperature-programming capability of LECO ONH836 instrument, herein we wish to demonstrate that by analyzing samples in different temperature modes (flash heating, ramping and stepped heating), it is possible to quantitatively speciate the O, N and H chemistries in powders, such as surface and interface oxygen, oxide precipitates, interstitial oxygen, surface -OH or physisorbed moisture, from % levels to ppm levels.

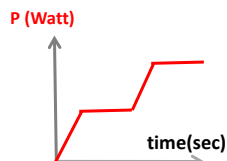
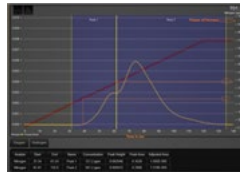
IGA Fractional Analysis Method Development – N in High Purity Graphite



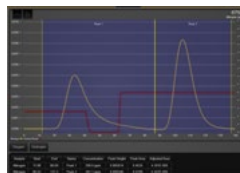
In flash mode the total N is determined



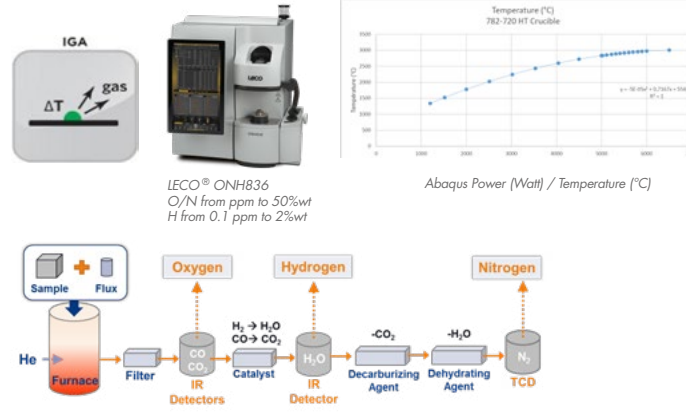
In ramp mode two N chemistries are identified



In steps mode the N chemistries are resolved and quantified

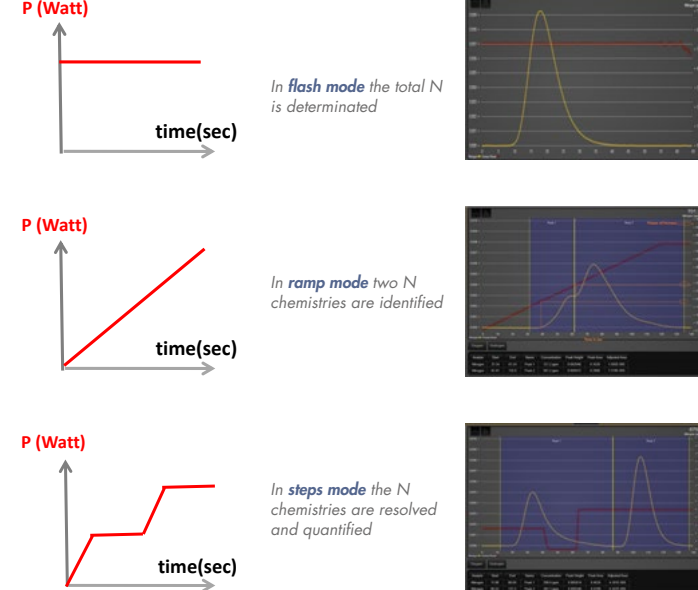


Instrument Operating Principle



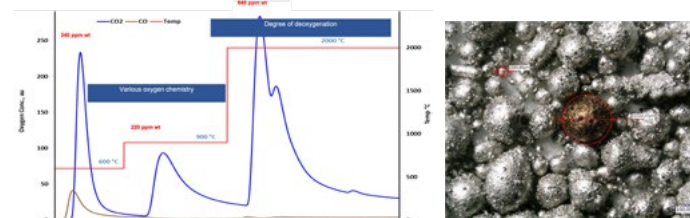
LECO® ONH836
O/N from ppm to 50%wt
H from 0.1 ppm to 2%wt

Abaqus Power (Watt) / Temperature (°C)



Case Study I: Fractional O Analysis of Ta6V Powder for Additive Manufacturing

Fractional O Analysis of Ta6V Powder



IGA fractional analysis gives:

- Information on various oxygen chemistries
- Surface oxygen/bulk oxygen ratio
- Quantitative and precise results

ELEMENT	H	O	N
AVERAGE, wt%	0.029	0.11	0.065
% RSD (n = 3-5)	4	10	12

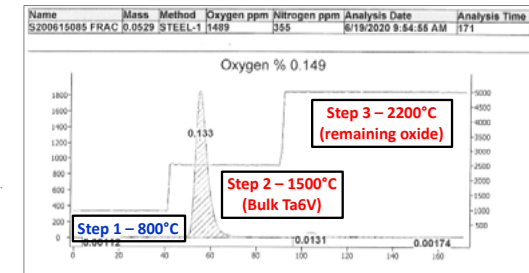
Comparative IGA Flash / Fractional

Operating Mode	REP. 1	REP. 2	REP. 3	AVG (ppmw)	RSD (%)
IGA Flash	3990	3850	3960	3930	1.9
IGA Fractional	1490	1430	1505	1475	2.6

The difference is attributed to moisture and M-OH bonds on the powder

Step 1 – 800°C

Step 1 is set to 800°C. This temperature step is high enough to drive off moisture and to dehydrate M-OH bonds, but low enough to prevent them from conversion to CO and CO₂ for IGA dosing.



Case Study II: Fractional O and H Analysis of Al Powder for Additive Manufacturing

ppmw	Lot A		Lot B		Lot C	
	O	H	O	H	O	H
IGA Flash	1855	66	2826	93	2091	81
IGA rampe	1539	39	2701	82	1743	52
Flash - rampe	316	27	125	11	348	29
H/O (%)	8.5%		8.8%		8.3%	

Since most H/O bonds exist in H₂O and M-OH form with stoichiometric ratios of 12.5% and 6.3%, it is estimated these lots contain ~35% H₂O and ~65% M-OH. Further characterization and verification can be done by determining moisture on LECO RC 612, surface oxide thickness with Auger Electron Spectroscopy for, O/H bonding chemistries with XPS and FTIR.



ANALYSIS OF TiC-BASED ALLOYS PREPARED BY MECHANICAL ALLOYING AND SPARK PLASMA SINTERING

Mohsen Mhadhbi | National Institute of Research and Physical-Chemical Analysis | Ariana, Tunisia
 Frédéric Schoenstein | Paris 13 University | Sorbonne Paris City, France
 Noureddine Jouini | Paris 13 University | Sorbonne Paris City, France

Introduction

The majority of the products composed of TiC-based alloys are fabricated according to traditional powder metallurgical technology like preparation of a mixture of TiC powder with metal binder, hot isostatic pressing, compaction of the mixture, forging, sintering and additional treatment [1]. Thus, to synthesis a homogeneous titanium carbide (TiC) and binder metal mixture, mechanical milling of the mixture is used. During this process, the physical, chemical, and mechanical properties of the starting components undergo changes. This influences the structure and properties of hard TiC-based alloys. However, the character of the interaction between the binder metal and titanium carbide effect the mechanical properties of TiC-based alloys [2]. These materials are used in several applications like biomedical, aircraft, cutting tools, etc.

Our work aims to analyse the proprieties of TiC-based alloys prepared by mechanical alloying followed by spark plasma sintering.

Experimental

Elemental powder mixtures of Ti (< 40 µm, 99.9%), W (1-5 µm, 99.9%), Zr (99.9%), Cr (99.9%) and carbon (99.9%) were sealed into a stainless steel vial with 5 stainless steel balls (1.5 mm in diameter and 1.4 g in mass) in a glove box filled with purified argon. The ball to powder weight ratio was 70:1. The mechanical alloying (MA) process was performed at room temperature using a high energy planetary ball mill (Fritsch, Pulverisette 7). Thus, the powders were milled for 20h. The obtained nanocrystalline powders were sintered using SPS-5155 SYNTEX apparatus under a pressure value of 80 MPa for 5 min. Before analysis, the obtained samples were polished using a polisher model PX 300. The microstructure and the morphology of the samples were studied by using X-ray diffraction (XRD) using X'Pert PRO MPD PANALYTICAL apparatus and scanning electron microscopy (SEM) using an FEI Quanta 200 environmental scanning microscope. The porosity of the samples was determined by using IA44 apparatus. Therefore, the Vickers hardness of the samples was measured by LV hardness tester. The results show that the samples have homogenous structure with a low porosity, a high relative density, and a high Vickers hardness.



Planetary ball Mill SPS-5155 SYNTEX apparatus Final product (bulk)

Results and Discussion

The synthesized powders obtained by milling and sintering are analyzed by various techniques.

X-Ray Diffraction analysis

Figure 1 illustrates the XRD patterns of the powders milled for 20h and sintered for 5 min.

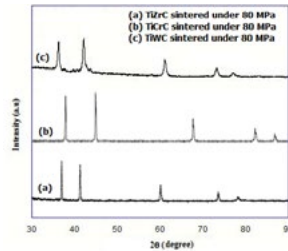


Figure 1. XRD patterns of TiC-based powders: (a) TiZrC sintered under 80 MPa, (b) TiCrC sintered under 80 MPa, and (c) TiWC sintered under 80 MPa

- Nanocrystalline phases were obtained for all the powders milled for 20h.
- The mean crystallite size, determined by the FullProf program using the Rietveld refinement, decreases with increasing milling time, on the other hand the mean microstrain increases with increasing milling time.

Scanning Electron Microscopy analysis

The SEM micrographs of the samples (powders) milled for 20h and sintered for 5 min are represented in the following figure 2.

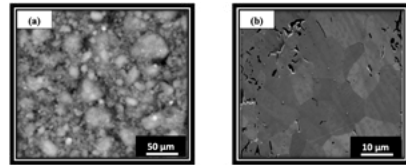


Figure 2. SEM micrographs of TiC-based powders: (left) milled for 20h and (right) sintered for 5 min

- By increasing the milling time up to 20h, the morphology of powders is still homogenous but with very fine agglomerated particles smaller than 1 µm in size.
- After sintering for 5 min, small pores are observed. In fact, the intergranular pores coalesced to form closed pores. Particles of different sizes agglomerate to form coarse grains, while heterogeneous distribution of equiaxed grains still occurs.
- Sintering process leads to the grain growth of the powder particles with retention of nanoscale.

Physical and Mechanical Properties

The experimental results including mechanical and physical properties are illustrated in Table 1.

TABLE 1: RELATIVE DENSITY, POROSITY, AND VICKERS HARDNESS OF PREPARED MATERIALS			
Material	Relative density (%)	Porosity (%)	Vickers Hardness (HV)
TiWC	98	5	2980
TiZrC	98	4	2765
TiCrC	97	5	2350

- The materials have an excellent physical and mechanical properties.
- Dense materials are obtained.
- The obtained materials are expected to replace the standard materials.

Conclusion

In this work, bulk nanocrystalline carbides were fabricated through mechanical alloying followed by spark plasma sintering. The mean crystallite size reach about 10nm after 20h of milling. The increasing of milling time decreases the temperature of densification. The sintered materials show excellent physical and mechanical properties. The density of the final products is 98% and the hardness is about 2800HV, which is greater than that of TiC carbides (2200HV). The maximum hardness was obtained for the more dense materials, meanwhile, the grain size is large. The hardness evolution doesn't follow the Hall-Petch behavior and is more affected by the material porosity.

[1] F. Eisenkolb, Powder Metallurgy, Technik, Berlin, 1955.

[2] D. Moscovitz and H.K Plummer, Proc. Int. Conf., Sci. Hard. Mater., No. 4, London, 1983, Jackson, pp. 299-309.

DEVELOPMENT OF A METHOD TO ANALYZE ALUMINUM ALLOYS POWDERS USING THE GAS ANALYZER LECO ONH836

Jimmy Dardinier | MetaFensch / Uckange, France
 Thibaut Turlan | IRT-M2P / Metz, France
 Agathe Deborde | MetaFensch / Uckange, France

Introduction

LECO methods exist to analyze oxygen (ONH836_O_ALUMINUM_203-821-459) and hydrogen (RHEN602_H_ALUMINUM_203-821-300) in aluminum. The goal of this work is to determine if a method able to analyze oxygen, nitrogen, and hydrogen in aluminum at the same time is feasible. Past work at MetaFensch has shown that ONH836_O-H_TITANIUM_HYDRIDE_203-821-458 (Oxygen and Hydrogen Determination in Titanium Hydride) can be used to analyze oxygen and hydrogen in titanium powders and also adapted to include nitrogen with good repeatability. For this reason, this method was taken as a starting point for development in aluminum.

Description of the initial method

The materials used to prepare the sample are shown in the table below. The powder sample (around 0.1 g) is placed along with graphite powder within a Nickel capsule and then put in a graphite crucible for melting and gas analysis.

Materials	LECO reference
Graphite crucible	782720
Nickel capsule	502-822
Graphite powder	501-073

Table 1: Reference of the additives used in the initial method.

Based on past experience with titanium powder, the addition of a tin pellet helps desorb nitrogen from the sample and also increases the volume in the crucible. The utility of this additional pellet for aluminum powder is a subject of investigation.

Furnace parameters and the heat cycle are listed below:

- 6000W for drying 3 times (1000w for 20sec)
- 100 seconds at 1200W
- An increase from 1200W to 4800W over 20 seconds
- A plateau at 4800W for 20 seconds

Starting from the initial method, the objective is to adjust parameters specifically for aluminum. Different levels of each parameter can be explored: heating power, powder quantity and the type/number of additives. To set these parameters, the following experiments were carried out:

- 5 measurements at different power levels to target the optimal power to melt aluminum powder
- 16 measurements with different quantity of powder
- 5 measurements to evaluate the impact of the additives (Ni capsule, Sn pellet and Graphite powder)

In this study, a new alloy powder for Additive Manufacturing was chosen to adjust the method.

About the authors

MetaFensch and IRTM2P have a joint research laboratory located in the northeastern France, working with industrial partners on materials and metallurgical R&D projects. In this laboratory, the characterization of oxygen, nitrogen, and hydrogen contents in titanium alloys (bulk materials and powders), using the existing "Oxygen and Hydrogen Determination in Titanium hybrid" method from LECO, has been studied. With the arrival of a new VIGA atomizer (Vacuum Induction Gas Atomization) dedicated to the study of light alloy powders, a need for aluminum powder characterization appeared. The development of a method dedicated to analyzing O, N, H contents in aluminum powders using LECO ONH836 has been carried out for this purpose.

Tests and results

Before each series of tests, a blank analysis is performed: 3 measurements without aluminum powder and without recording the results in order to heat the machine up and increase stability.

Power

To investigate the power needed to melt aluminum powder, 5 different levels were tested: 3500W, 4000W, 4800W, 5200W and 6000W. The other parameters were fixed: powder quantity (0.10g) and additives (1 Sn pellet, 1 Ni capsule and 0.5g of Graphite powder).

Titanium or tungsten powders require 4800W to melt, a lower power is thus expected for aluminum, as the melting temperature is lower. The results of the test are shown in Figure 1.

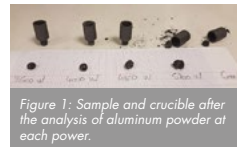


Figure 1: Sample and crucible after the analysis of aluminum powder at each power.

To evaluate the optimal power, the sample after analysis is observed. The materials within the crucible (aluminum powder + additives) need to be perfectly melted, resulting in a spherical shape with no remaining free powder. A melting temperature that is too high leads to degradation of the crucible.

At 5200W and 6000W, cracks are observed on the crucible and the base has eroded or even become detached from the crucible. At 3500W melting is not quite complete while the sample is deteriorated at 4800W. Therefore, 4000W seems to be optimal, with a good melt and an undamaged crucible.

Powder quantity

To obtain good reproducibility, an optimal sample quantity is needed: if there is not enough powder, dispersion within the results increases, whereas too much powder leads to incomplete melting and, therefore, erroneous results. To determine the quantity of powder necessary to produce representative results, 16 tests with increasing amounts of aluminum powder were performed: from 0.05g to 0.20g, in steps of 0.01g. The precision of the scale is 0.001g. The other parameters were fixed: power at 4000W and additives (1 Sn pellet, 1 Ni capsule and 0.5g of Graphite powder)

The oxygen content is used to compare the results and study the influence of sample quantity.

The oxygen level and the shape of the melted sample obtained for different quantities of aluminum powder are shown in Figure 2.

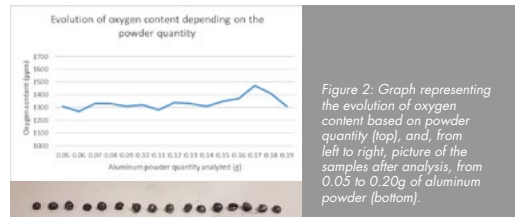


Figure 2: Graph representing the evolution of oxygen content based on powder quantity (top), and from left to right, picture of the samples after analysis, from 0.05 to 0.20g of aluminum powder (bottom).

Apart from 2 measurements with higher mass, the oxygen content remains approximately 1300ppm. Therefore, the quantity of powder has no major influence on the analysis. Considering this observation, it is decided to use a mass sample of 0.1 +/- 0.01 g for the analysis of aluminum powder (as is recommended in the LECO method: Oxygen and Hydrogen in Titanium hydrid).

Additives

The next step is to analyze the impact of additives. Measurements were carried out with varying the number of additives: tin pellet, graphite powder and nickel capsules. The other parameters were unchanged, powder quantity of 0.1g and power of 4000W

The average values obtained after analysis are presented in Table 2 below, and the picture of the samples to observe the melt is in Figure 3.

in ppm	Additives	Oxygen	Nitrogen	Hydrogen
Oxygen and Hydrogen Determination in Titanium Hydride (LECO)	1 Sn pellet 0.5g of graphite powder 1 Ni capsule	1310 +/-26	16 +/-1	23 +/-7
Without Graphite powder	1 Sn pellet 1 Ni capsule	1330 +/-11	16 +/-1	19 +/-9
Without Tin pellet	0.5g of graphite powder 1 Ni capsule	1140 +/-68	18 +/-1	14 +/-1
Ti method with 2 Tin pellets	2 Sn pellets 0.5g of graphite powder 1 Ni capsule	1350 +/-16	17 +/-1	21 +/-2
Ti method with 2 Nickel capsules	1 Sn pellet 0.5g of graphite powder 2 Ni capsules	648 +/-870	17 +/-1	30 +/-7

Table 2: Results of O, N, H contents with different additives (type and number).



Figure 3: Sample aspect after analysis with different additives, with 2 tin pellets for the 2 samples on the left, and 2 Nickel capsules for the 2 samples on the right.

Comparison using the Titanium method as a reference was carried out; the additives for this method are 1 Ni capsule, 1 Sn pellet and 0.5g of graphite powder. Removing the graphite powder makes no difference in the O, N, H results for aluminum. On the contrary, removing the tin pellet disturbs the measure by decreasing oxygen content and increasing result spread. Tin pellets can thus be considered to play a role in measurement accuracy. Increasing the number of pellets from 1 to 2 does not have any significant influence, therefore, 1 pellet is sufficient.

Nickel capsules cannot be eliminated as they are used to contain the aluminum powder before melting. Nevertheless, a method with an addition of Ni capsule is not relevant, as it deteriorates the measurement of oxygen (600 ppm vs. 1300 ppm expected) and leads to melting problems, as it is shown in Figure 3.

Comparison with certified materials and laboratory

Finally, to verify that the method is correct, 2 certified reference materials, where dissolved gas levels are already known, were tested. Using the aluminum method developed, the following results were obtained (Table 3).

Certified reference materials	in ppm	Oxygen	Nitrogen	Hydrogen
502-876 (N°0300)	Target (certified)	3070 +/- 50	60 +/- 10	17.3 +/- 3.2
	Mean value (3 measurements)	3050 +/- 35	91 +/- 2	19.3 +/- 2.7
502-867 (N°0739-1)	Target (certified)	1380 +/- 50	120 +/- 10	(25.4)
	Mean value (3 measurements)	1340 +/- 20	99 +/- 4	23.8 +/- 5.1

Table 3: Analysis of CRMs using the method developed in this study

Comparing obtained measurements with CRM standards, it can be seen that average oxygen and hydrogen contents are within standard deviation. However, this is not the case for nitrogen. Measurements can be used qualitatively to determine trends but further work is required in order to improve accuracy. To consolidate the relevance of the developed method, measured oxygen content on 2 aluminum alloy powders has been compared to a certified laboratory (Table 4).

in ppm		Oxygen content (3 measurements)			Mean	Standard deviation
Certified lab	Al Powder 1	1200	1400	1400	1300	89
MetaFensch	Al Powder 1	1130	1100	1070	1070	64
Certified lab	Al Powder 2	470	490	310	430	76
MetaFensch	Al Powder 2	270	300	330	300	25

Table 4: Comparison of Oxygen contents for 2 Al powders, measured by MetaFensch with the new method and a certified laboratory.

The comparison of these results is quite good within the current calibration interval (range from 1000 to 3000ppm). To further improve the method and measure lower oxygen content in aluminum powder (< 1000ppm, as for sample Al powder 2 in Table 4), a lower oxygen content reference material is required.

Conclusion

The titanium method previously developed corresponds to a high temperature crucible, a tin pellet, approximately 0.5g of Graphite and a capsule of Nickel, for a titanium powder sample of 0.1g (+/- 0.015g) with an optimal furnace parameters and heat cycle. A parametric study was carried out to adjust this method for aluminum.

The results show that the use of graphite, which lowers the melting point of titanium in the original method, is not critical for aluminum. Experiments also show that the amount of tin required is 1 pellet and a standard nickel capsule, in order to ensure a good melting of the sample. Figure 4 summarizes these findings.

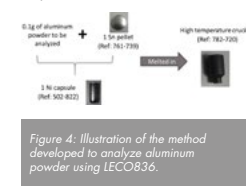


Figure 4: Illustration of the method developed to analyze aluminum powder using LECO836.

LECO SC632 ANALYZER

LECO boat crucible as an aid to analysis of Total Organic Carbon (TOC) content in rock samples

Doaa A. Mousa | Exploration Department / Egyptian Petroleum Research Institute (EPRI), 1 Ahmed El Zomor St. Nasr City, Cairo, 11727, Egypt
Shereen A. Naseef | Exploration Department / Egyptian Petroleum Research Institute (EPRI), 1 Ahmed El Zomor St. Nasr City, Cairo, 11727, Egypt
Amr M. Shehata | Exploration Department / Egyptian Petroleum Research Institute (EPRI), 1 Ahmed El Zomor St. Nasr City, Cairo, 11727, Egypt

Introduction

The Total Organic Carbon (TOC wt%) is a very important parameter, it plays an essential role in the evaluation of source rock generating potential of petroleum in the sedimentary rock. In Egyptian Petroleum Research Institute, we use the LECO SC632 analyzer that is best in this application and recommended by most of the workers. In addition to TOC, the instrument measures the Total Sulfur (TS) and Total Carbon (TC). The results are precise every-time after an easy calibration step. The machine is made for heavy duty work and has a nice easy to handle digital interface.

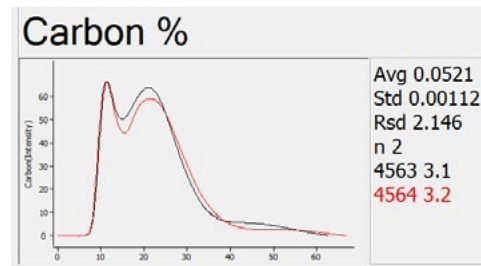
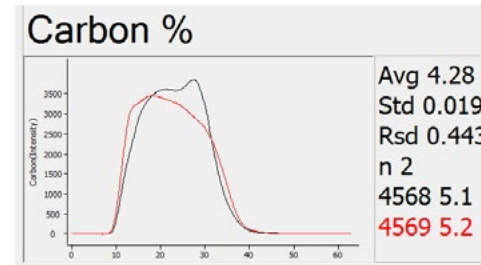
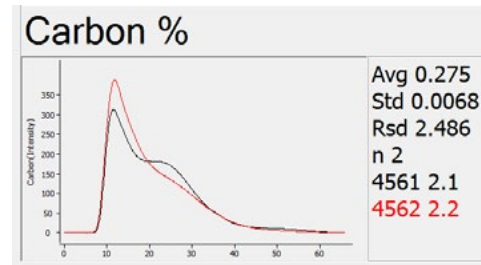
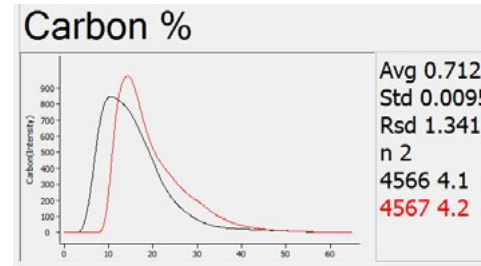
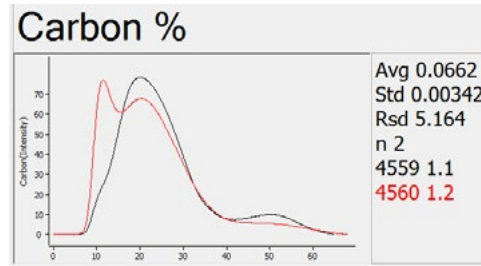
Using the LECO Crucible 528-203-250 BOAT CRUCIBLE ZIR and the application note by LECO for Sulfur and Carbon in Cement, Fly Ash, Limestone, Soil and Ore, in determining the Total Organic Carbon (TOC) content it is very important in our laboratory work.

Method

The method is simply summarized as follows:

- 1) The fine ground dried sample is weighted according to the application recommended weight in clean boat crucible.
- 2) The sample is treated with 10 N HCl acid to remove any inorganic carbon content.
- 3) The excess of HCl seeps through the pores of the boat crucible.
- 4) The sample with the boat is washed with distilled water to remove any access of HCl acid then dried in the oven at 105 °C.
- 5) The samples are mixed with com cat as recommended in the application note, then analyzed in the LECO SC632 for complete combustion.
- 6) The TOC content is determined.
- 7) Another batch of the samples is treated in glass watch with the same procedures and the residue is totally moved to clean crucible after drying, mixed with com cat, then analyzed in the LECO SC632 for complete combustion.

The experiment is applied here on five (5) rock samples with different composition and different TOC content. The results are very similar as shown in figs. (1-5). Each figure has two curves, each one represents one method. The first is applied by using the LECO crucible (black curve), the second represents the second method in glass watch (red curve).



LECO SPECTRUM SYSTEM 2000

LECO Spectrum System 2000 polishing and grinding machine

Walid A. Makled | Exploration Department / Egyptian Petroleum Research Institute (EPRI) | 1 Ahmed El Zomor St. Nasr City, Cairo, 11727, Egypt

Overview

The LECO Spectrum System 2000 is a robust grinding and polishing machine that was designed for preparing the metallurgical polished section for microscopical studies. In the Egyptian Petroleum Research Institute, we have this monster machine for more than fifteen years. The machine is fully automatic with easy to handle digital interface. The machine works perfect with minimum maintenance processes and easy replaceable spare parts and consumables.



1. LECO Spectrum System 2000 in EPRI laboratory

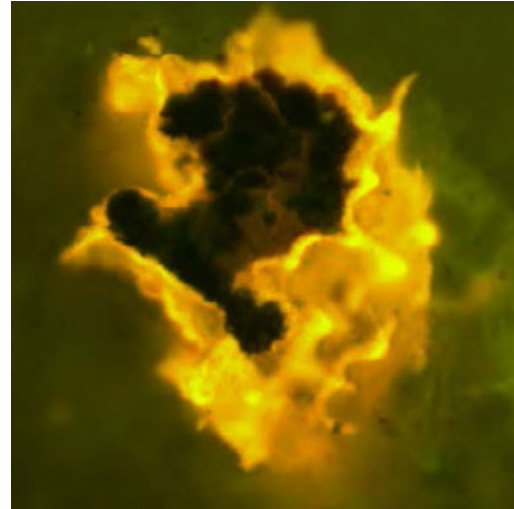
Conclusion

However, we use the machine to polish the soft and hard rocks for the purposes of the microscopical studies in the field of sedimentology and organic petrography. In organic petrography, a polished relief-free sample surface is required to measure light reflectance from the organic particles (Vitrinite) in the matrix of mineral grains. The vitrinite reflectance is the main parameter to assess the thermal maturity of the organic matter in the rock samples and their potential to generate petroleum.

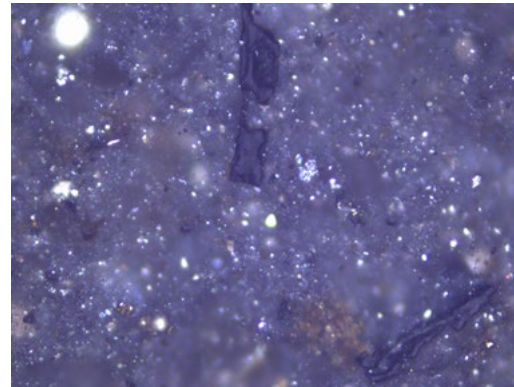
According to the method and polishing sequence we designed for processing the samples in our lab, the Spectrum System 2000 machine produces flawless rock briquettes that comply with the ASTM preparation method. We believe that the efficiency of the polishing process can be improved if the machine is supplied with grinding and polishing discs that are specifically customized to confront the fragile nature of soft shale samples. The samples of soft shale require special precaution during the grinding and polishing to avoid grain loss can cause relief and pits. The pits cause many problems during the measuring of the reflectance and produce many errors in the results.



2. Rock sample pellet under the microscope



3. Organic matter in fluorescence mode



4. Notice the vitrinite particles with grey color reflectance in white light



PRETREATING LIGNOCELLULOSIC BIOMASS WASTES FOR THE NEXT GENERATION OF SOLID FUELS

Karl Hornsby^{1,2}, Martin J. Taylor^{1,2}, Peter Hurst³, Simon Walker⁴ and Vasiliki Skoulou^{1,2*}

¹ Energy and Environment Institute, University of Hull, Cottingham Road, Hull, HU6 7RX, United Kingdom

² B³ Challenge Group, Department of Chemical Engineering, University of Hull, Cottingham Road, Hull, HU6 7RX, United Kingdom

³ Biorenewables Development Centre (BDC), Chessingham Park, Dunnington, York, YO19 5SN, United Kingdom

⁴ Jesmond Engineering Limited, Brough Business Centre, Skills Lane, Brough, HU15 1EN, United Kingdom

* Corresponding author: V.Skoulou@Hull.ac.uk

Abstract

To assist in the measures to combat climate change and considerably reduce the use of fossil fuels, three abundant lignocellulosic biomass wastes have undergone physicochemical pre-treatments to reform them into alternative solid fuels. By leaching wheat straw, barley straw and bagasse waste, there has been a profound effect on their calorific values and lowering of their mineral (ash) content without sacrificing their carbonaceous structures. It was found that by water washing over 24 h at 50 °C, the calorific values of wheat straw and barley straw increased by 10% and 14%, respectively, as a result of their de-ashing.

Introduction

As we move away from fossil fuels we endeavour to find alternative solid fuels. One such possibility is the upgrading of the underutilised lignocellulosic biomass wastes. A carbon neutral approach that can be adapted and optimised to assist in both the impending energy crisis, and averting climatological disaster caused by carbon emitting processes. By characterising and pre-treating a range of feedstocks, a more varied group of lignocellulosic biomass options can be made available for the Energy to Waste (EiW) industry. However, these solid wastes are not drop in fuels. To unlock their true potential they must be physically, chemically or physicochemically pre-treated to reform them into non-problematic solid fuels.^{1,2} One such option is leaching, otherwise known as water washing. This is where a waste material is immersed in water and mixed at a variable speed and temperature. Here, the water will enter the material and exit carrying dissolved mineral ions into the liquid phase. As a result, the ash content of lignocellulosic biomass wastes can be radically lowered.³ Ash, specifically elements such as K, Na, Mg, S and Cl are major culprits for damage to thermochemical reactors. Various inorganic deposits can adhere to the reactor walls which have been proven corrosive and create issues with reactor heat transfer. Additionally, during Fluidised Bed (FB) operation of industrial scale EiW technologies, low melting point eutectic mixtures can form which will interact with the bed material and cause de-fluidisation. This is where the FB reactor is forced to shutdown, as eutectic mixtures cause bed material fusing which restricts gas flow, proceeding via a sudden pressure drop inside the

biorenergy system. To determine the extent of de-ashing, the LECO TGA 701 (Figure 1) was employed due to its versatile nature and the ability to process a high sample throughput. Moreover, by handling a large sample size (~1 g) a more representative sample can be processed than commonly used in smaller scale instruments.

Materials preparation

Three lignocellulosic biomass wastes; wheat straw, barley straw and bagasse were blended in a Knife mill (Retsch GM 200) for 1 min at 10,000 rpm. The resulting powders were separated and the 1.2 mm fraction was retrieved using a Retsch AC 200 sieve stack. Each feedstock particle size was then leached in deionised water at a ratio of 10g/L at 50 °C and 400 rpm for 24 h. The slurry was separated and dried under *vacuo* before drying in a Fisherbrand Gravity Convection Oven at 105 °C for 24 h, according to ASTM standards.

Feedstock characterisation

Fourier Transform Infrared (FTIR) spectra were obtained using a Thermo Scientific Nicolet iS5 with a PIKE MIRacle single reflection horizontal ATR accessory (Figure 2). Scanning Electron Microscope (SEM) images were acquired via a Zeiss EVO 60 instrument at a pressure of 10⁻² Pa and an electron acceleration voltage of 20 kV (Figure 3). Raw and leached samples were adhered to a coated conductive carbon tape and attached to the specimen holder, where a 10 nm thick coating of graphite was added to the surface. Bomb calorimetry was carried out using a Parr 6200 Isothermal calorimeter.

Parallel feedstock processing

To maximise the data quality and acquisition six, ~1 g samples of raw and leached waste were analysed per heat cycle. A standardised LECO procedure for biomass was used consists of a moisture phase in air from ambient to 107 °C at a rate of 3 °C/min. Holding for several minutes before adding crucible lids for the removal of volatiles. This stage was carried out under N₂ from 107 °C to 950 °C at 5 °C/min, holding for 7 min before cooling to 600 °C. After the lids were removed the ashing phase was carried out in air from 600 °C to 750 °C at 6 °C/min before cooling to ambient conditions, the proximate analysis for each feedstock is summarised in Table 1.

Results and Discussion

Table 1 shows the effect of water washing on the three lignocellulosic biomass wastes. It is clear that the ash has significantly reduced across all feedstocks as result of water washing. Specifically, 71% for wheat straw, 72% for barley straw and 45% for bagasse. The straw feedstocks, known for their high K and other water soluble elements benefited from the leaching pre-treatment. Whereas leaching was not as efficient for bagasse, known for its high Fe and Al content. This being said, Fe is not a known element for causing eutectic mixtures, instead known for its catalytic properties for gasification.⁴ This being leaching has benefited an increase in heating values (HHV) for all feedstocks, specifically for wheat and barley straws.

Feedstock		Moisture (wt %)	Volatile (wt %)	Fixed Carbon (wt %)	Ash (wt %)	HHV (MJ/Kg)
Wheat Straw	Raw	7.67	71.68	16.55	4.11	16.99
	Leached	2.90	79.66	16.23	1.21	18.15
Barley Straw	Raw	10.06	70.20	16.60	3.13	16.79
	Leached	3.88	79.63	15.61	0.88	17.63
Bagasse	Raw	6.63	76.19	15.78	1.52	17.41
	Leached	3.18	81.21	14.65	0.84	17.76

FTIR spectra shown in Figure 2 all show for the most part there is negligible structural differences between raw and leached feedstocks, indicating that carbonaceous matrix is mostly unchanged. However, a mild decrease in a feature at 1600 cm⁻¹ for wheat straw does indicate that the leaching process has carried out some delignification. Additionally, for both barley and wheat straws, a change to the double feature at 2900 cm⁻¹ indicates that some of the cellulose linkages have been hydrolysed.

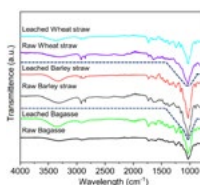


Figure 2: Stacked FTIR spectra showing a lack of structural alteration before and after leaching, for all feedstocks.

Figure 3 shows SEM images for both raw and treated wheat straw (Figures 3a and 3b), barley straw (Figures 3c and 3d) and bagasse (Figures 3e and 3f). All images were taken at the same magnification and show the effect of leaching over 24 h. The surface morphology for all feedstocks appears to have changed. This can be in the form of cracking or separating or through ruptures in the feedstock wall. It is believed that these surface opening could prove beneficial for gas diffusion throughout the feedstock during thermochemical conversion. Surface ruptures appeared to be more apparent for barley straw and bagasse. This is evidenced in Figures 3d and 3f where high contrast dots have appeared along the channels. This being said, the surface morphologies are relatively similar across the feedstocks.

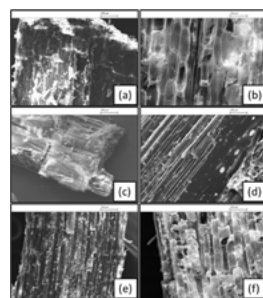


Figure 3: SEM images of (a) Raw Wheat straw, (b) Leached Wheat straw, (c) Raw Barley straw, (d) Leached Barley straw, (e) Raw Bagasse and (f) Leached Bagasse.

The upgraded waste feedstocks once leached represent better solid fuels. This is because of their clean decrease in ash content (Table 1) and no major decrease in carbon structure (Figure 2). To further characterise these materials bomb calorimetry was carried out, as shown in Figure 4a and a further inspection into the DTG curves produced during thermogravimetric analysis (TGA) (Figures 4b and 4c). The information supplied by these curves informs how the structure of the material has changed after the pre-treatment of leaching and if there is greater overall mass loss at a given temperature. Figure 4a shows that the calorific value of each feedstock has changed after leaching. For wheat and barley straw this has been a positive alteration where an increase in calorific value of 10% and 14% are shown, respectively. Bagasse on the other hand, although possessing less ash has suffered from a negative effect by 5%. This being said, data from the LECO TGA 701 has shown that bagasse has a larger maximum mass loss at 350 °C than the other feedstocks both raw and leached. Additionally, due to the fine temperature control across all samples, Figures 4b and

4c show two distinct peaks for each feedstock, the first at ~270 °C and the second between 300-350 °C. These peaks are indicative of depolymerisation of hemicelluloses and pectins (initial peak) and the degradation of cellulose (major peak).

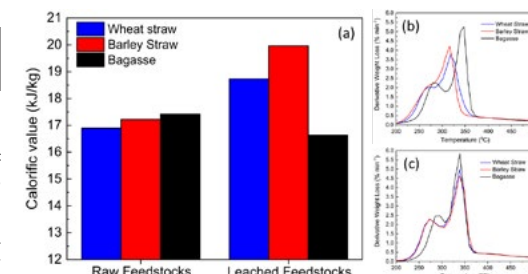


Figure 4: (a) Bomb calorimetry of raw and leached feedstocks, (b) DTG curves for all raw feedstocks and (c) the effect of leaching on the DTG curves for each feedstock.

Conclusions

In the quest to find alternative solid fuels to replace existing fossil based fuels, three different feedstocks provide an option after pre-treatment for ash removal. By using a cheap and scalable technology such as conventional water leaching, it has been found to remove a large quantity of the undesirable ash components from cereal straws and bagasse. As a result, improving the heating value and for the straws their calorific value by over 10%. Due to a relatively low temperature used for the leaching pre-treatment, there was no large loss of sugar content from the feedstocks, as shown by FTIR. Ultimately demonstrating that leached barley straw is a strong contender for the future, when not used in competitive markets, due to its low ash content and higher calorific value. Bagasse however is the weakest feedstock under the conditions shown due to its high ash content and low calorific value.

Acknowledgements

All authors are greatly acknowledge the THYME project (UKRI, Research England) for funding. We would like to especially thank Mr Timothy Dunstan for the acquisition of HRSEM images and Jesmond Engineering for fruitful discussions.

References

- Taylor, M. J.; Alabdrabalaameer, H. A.; Michopoulos, A. K.; Volpe, R.; Skoulou, V., Augmented Leaching Pretreatments for Forest Wood Waste and Their Effect on Ash Composition and the Lignocellulosic Network. *ACS Sustainable Chemistry & Engineering* 2020, 8 (14), 5674-5682.
- Taylor, M. J.; Alabdrabalaameer, H. A.; Skoulou, V., Choosing Physical, Physicochemical and Chemical Methods of Pre-Treating Lignocellulosic Wastes to Repurpose into Solid Fuels. *Sustainability* 2019, 11, 3604.
- Alabdrabalaameer, H. A.; Taylor, M. J.; Kauppinen, J.; Soini, T.; Pikkariainen, T.; Skoulou, V., Big problem, little answer: overcoming bed agglomeration and reactor slagging during the gasification of barley straw under continuous operation. *Sustain Energy Fuels* 2020.
- Skoulou, V.; Zabanitoulou, A., Fe catalysis for lignocellulosic biomass conversion to fuels and materials via thermochemical processes. *Catalysis Today* 2012, 196 (1), 56-66.

Moisture, Volatiles and Ash in Biofuels with the TGA801

Michael Jakob | European Field Product Manager Analytical Product Line | LECO EUROPE

Overview

Moisture, Volatiles and Ash are some of the most important parameters determined in the characterization of biofuels. Generally those parameters are determined by the thermogravimetric behavior of the samples at different temperatures and in different atmospheres. Moisture determination is done according to suitable standard procedures at temperatures of approximately 105°C. Ash determinations are made at 550°C, or higher temperatures. The measurement of the so-called Volatiles is a technical parameter determined by measuring the amount of sample released at higher temperatures without burning/oxidizing. So generally this is determined in an inert (Nitrogen) atmosphere and at a fixed temperature and time period. In most cases this time period is 7 minutes and the temperature above 900°C.

Analytical Parameters

The LECO TGA 801 is a special thermogravimetric analyzer that has been developed for the determination of Moisture, Volatiles and Ash content of solid fuels. Nineteen (or thirty-eight) samples, with sample weights of up to 5 g can be analyzed simultaneously. All 3 parameters are analyzed in one run, just by running one step after the other. The system is fully automated, so only sample input has to be done manually.



Figure 1: LECO TGA 801 with ceramic turntable and crucibles.

Moisture, Ash and Volatile determination can be done according to the ISO standards 18123, 18122 und 18134. According to these standards moisture, volatiles and ash are determined at different temperatures.

Automated systems can be used for determination of these parameters if it can be shown that the results match the results of the ISO methods.

Biofuel Moisture and Ash values from the automated TGA method and the manual ISO methods are expected to be the same because of the close similarity in the procedures. However, there is a procedural difference between the TGA and ISO methods for Volatiles. Both methods record the mass loss for a certain number of minutes at 900°C, but the TGA needs additional time for heating up the system from the moisture step (~105°C) to the volatile temperature of 900°C.

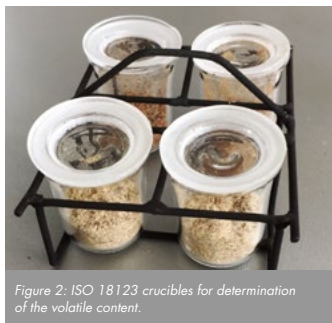


Figure 2: ISO 18123 crucibles for determination of the volatile content.

In this paper the moisture, ash and volatiles results from the ISO methods and those from the automated LECO TGA 801 method for different biofuels and waste materials are compared. In addition, different wood chips, peat samples, coal samples and plastic waste results are also compared for moisture, volatile and ash contents. The samples were analyzed using a LECO TGA 801 system, and the cited ISO procedures. The wood chips were ground with a mill, and the peat coal and plastic samples had been prepared for analysis using appropriate procedures.

	WP 1	WP 2	Peat 1	Peat 2	Coal 1	Coal 2	Plastic 1	Plastic 2
M TGA	5.71	5.12	2.72	2.78	1.25	2.31	<0.1	<0.1
M ISO	5.75	5.15	2.73	2.75	1.22	2.33	<0.1	<0.1
Ash TGA	1.60	5.69	4.29	6.39	7.37	11.99	11.87	8.74
Ash ISO	1.62	5.63	4.32	6.30	7.32	11.93	11.80	8.79

Table 1: Moisture (M) and Ash results from ISO and TGA procedures for various samples. Wood pellet (WP) and Ash values are reported on a dry basis.

As shown in Table 1 the average moisture and ash values for all of the samples agree very well. This behavior had been expected, because procedures and temperatures for the ISO and TGA programs are more or less the same.

	WP 1	WP 2	WP 3	WP 4	WP 5
Vol TGA	80.33	79.17	76.26	80.07	84.39
Vol ISO	79.72	78.59	77.32	80.61	84.26
Difference	0.61	0.58	-1.06	-0.54	0.13

Table 2: Volatile (Vol) results from ISO and TGA procedures for Wood pellet (WP) samples reported on a dry basis.

A comparison of the data for Volatiles from the wood pellet biofuel samples shows a linear relationship between the Volatiles results using the ISO method and Volatiles results using the TGA method with a "goodness of fit" or R² of 0.94. The maximum delta between both methods is 1.06 % and the average difference is 0.1 %.

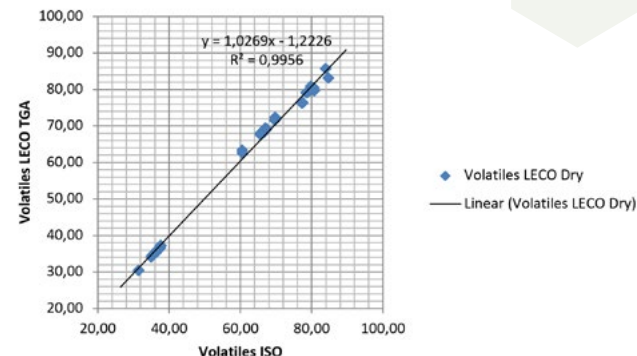


Figure 3: Comparison of Volatiles ISO Method / LECO TGA Method for coal, wood and peat samples.

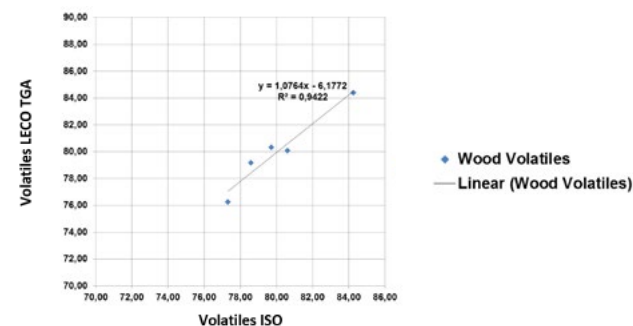


Figure 4: Comparison of Volatiles ISO Method / LECO TGA Method for wood samples only

Conclusion

The LECO TGA 801 is able to analyze beside moisture and ash also volatiles in solid biofuels with a very good coincidence to the ISO methods for solid biofuels. Any additional data handling parameters like calibrations or adjustments are not necessary. The advantage of having all 3 proximate analysis parameters determined automatically is obvious: automation, data security, convenience, and throughput.

VOCs FROM WOOD FIBERS INSULATION MATERIALS

VOCs from low density fiberboard measured with LECO PEGASUS® BT GC-TOFMS equipped with thermal desorption unit TD3.5+ and CIS as a cryo-focusing trap and a temperature programmable GC inlet.

Dorota Fuczek, Jarosław Szuta, and Krystian Szutkowski | STEICO Sp. z o.o.; Czarnków, Poland

VOCs in the indoor AIR

Nowadays the majority of people spend 90% of their lives in buildings - houses, schools, factories, offices, shopping centers, etc. That is why indoor air quality has a major impact on our health. Timber insulations help to control the internal environment of buildings. Steico within its products ensures keeping cold out, buffering external heat, regulating moisture content but also helping to promote breathable and healthy structures. Someone may ask, but thermal insulation products are not usually directly exposed to indoor air? After all, they are covered by different materials such as plasterboards, wood, bricks, or concrete, and that potential emissions from the insulation materials cannot get in contact with the indoor air. Nevertheless, the covering layers may not be gas-tight or may be perforated for the installation of technical building systems. And what is also important, the building owners have the right to be informed about the potential hazards connected to the insulation and construction materials used in his building.

To meet the needs of Steico product users, a volatile organic substance (VOC) emission measurement laboratory was established in the company's structure, thanks to which Steico has even greater control over processes and products. The laboratory has been equipped with modern apparatus - gas chromatography and mass spectrometry - LECO Pegasus BT GC-TOFMS. With the additional thermal desorption unit TD3.5+ connected directly to the GERSTEL Cooled Injection System (CIS), which is used as a cryo-focusing trap and as a temperature programmable GC inlet it is possible to measure VOCs from wood-based materials according to ISO 16000 and EN 16516.

Are we always aware of what is in the air we are surrounding ourselves with? It is easy to ignore harmful chemicals known as Volatile Organic Compounds (VOCs) as they are invisible, but long-term exposition to VOCs can cause serious illnesses. Steico focuses not only on the physicomechanical parameters of its products but also ensures low emissions from the wood fiber insulation material. Nowadays due to the running project co-funding within sectoral program Woodinn implemented by the National Centre for Research and Development (NCRD) within Operational Program Smart Growth 2014-2020, works, on a new generation, low-density insulation material for traditional and pole buildings, are carried out.

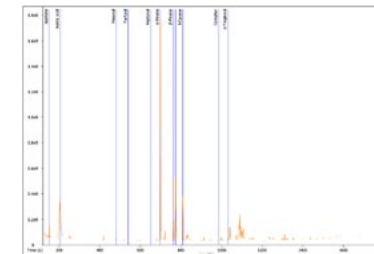
During the project implementation using the LECO Pegasus BT GC-TOFMS, solutions were integrated and developed that further reduce VOC emissions from insulation materials. The wood volatile constituents can more easily escape from a new board due to its very low density (around 80kg/m³). Therefore, during the work on this product, special care was taken to ensure that the emissions from it are also at a level that is safe for the user, as in the case of other Steico products. For this reason, when implementing the project, great emphasis was placed on the selection of such raw materials, as well as the adjustment of production parameters such that the emission from the new final product was also on a very low level.

Due to the fact that wood fiber insulation materials are around 80% made of pine wood, it can be expected that the main emitting substances from fiberboard are of natural origin such as for example terpene compounds, α and β -pinene, Δ^3 -carene, monocyclic monoterpenes such as limonene, β -phellandrene, terpinolene, and aromatic compounds like p-cymene. During the production of wood fiberboard, pinewood is subjected to hydrothermal treatment which leads to the creation of aldehydes formed by the autoxidative splitting of free unsaturated fats and fatty acids. By selecting the appropriate production parameters of the defibration of the wood, drying of the wood fibers, and pressing of the wood fiber insulation materials it is possible to minimize decomposition of wood.

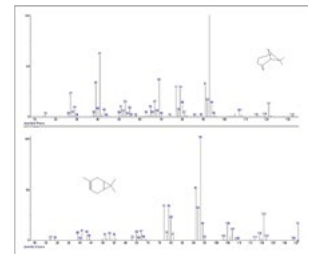
Additionally, for the production of low-density fiberboard in dry technology, it is necessary to use adhesive, hydrophobization agents, and in the case of a board with very low density, fire retardants which can also influence emission from the product. It is proven that lowering the pH of the environment leads to the intensification of emissions from products. Therefore, it is of great importance to select chemicals that in contact with natural wood will have the least possible impact on its decomposition and thus on the emission of undesirable substances. The developed chromatographic methods enable the control of individual raw materials before their use for production.

The LECO Pegasus BT GC-TOFMS equipment using the headspace technique allowed the capture of propylene carbonate in the adhesive at an early stage of raw material control. The knowledge gained, thanks to the thorough analysis and control of raw materials, in this case the binder, allowed to minimize or even eliminate the emission of propylene carbonate from finished products.

The research carried out in the Woodinn project has made it possible to minimize emissions even further from such natural insulation materials as Steico products by optimizing the input raw materials and the technological process itself. The use of LECO Pegasus BT GC-TOFMS equipment allows not only for quick reaction already during the control of the raw materials themselves as well as during changes in the process, but also allows for continuous development and improvement of insulation materials.



5. VOCs from low density fiberboard



6. Evaluation of VOC based on the mass spectrum



1. LECO Pegasus BT GC-TOFMS

2. Steico VOCs laboratory



3. From round wood to fibers - wood preparation

4. Production of low density fiberboard LDF



ANALYTICAL PYROLYSIS COUPLED WITH CHEMOMETRIC METHODS

In solid biofuels control and detection of illegal waste combustion in domestic boilers

Marcin Sajdak, Roksana Muzyka, Maciej Chrubasik
Institute for Chemical Processing of Coal, Zamkowa 1, 41-803 Zabrze, Poland

Aim

The main objectives of the research were to determine the possibility of applying the analytical pyrolysis coupled with chemometric methods such as clustering analysis (CA), principal component analysis (PCA), and classification and regression trees (C&RT) to quality control of solid biofuels such as biomass pellets, torrefied biomass, biochar and detection of illegal waste combustion in domestic boilers.

The material used in the study



1. Mix of biochar and kraft lignin, peat and lignite
2. Contaminated biomass pellet
3. Ash sample from domestic boilers

Analytical pyrolysis (Py-GC-TOFMS)

Pyrolysis-gas chromatography-mass spectrometry (Py-GC-TOFMS) was used to determine the pyrolysis behaviours of different three type of studied materials:



4. LECO Pegasus 4D

- biochars mixed with fresh low-rank fuels,
- contaminated biomass pellet,
- ash sample obtained by combustion of coal and plastics waste

Py-GC-TOFMS experiments were performed using a PEGASUS® 4D (LECO) equipped with a thermo-desorption unit (TDU, Gerstel), pyrolysis module (Pyro, Gerstel) and cooled injection system (CIS-4, Gerstel). Pegasus 4D is a comprehensive two-dimensional GC-TOFMS system. For this study, the instrument was switched to one-dimensional mode.

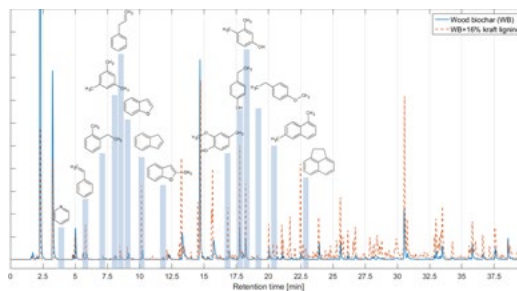
MATLAB in Py-GC-MS data processing

Raw Py-GC-MS data was processed using the MATLAB software. In the first step, chromatographic data have been subjected to the bases line correction by applying MATLAB baseline script. The next step in pre-processing raw chromatographic data was retention time correction (by icoshift MATLAB script).

Chemical markers indicating the contamination by external fuels of biochar

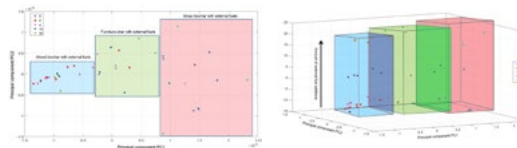
Chemical Component	External Fuel Additives		
	Kraft lignine	Peat	Lignite
Pyridine		+	
Styrene	+	+	+
Benzene, 1-ethyl-2-methyl-	+	+	+
Mesitylene	+		+
Benzene, 2-propenyl-	+		+
Benzofuran	+		+
Indene	+	+	+
Benzofuran, 2-methyl-	+		+
Creosol	+		+
Phenol, 4-ethyl-	+		
Phenol, 3,4-dimethyl-	+		
Benzene, 1-ethyl-4-methoxy-	+		
Naphthalene, 1,6-dimethyl-			+
Acenaphthene			+

5. Chemical markers from different biochar contaminates



6. Chromatographic comparison of pure biochar and after contamination by kraft lignin

Principal component analysis (PCA) in a quick method of contamination detection in biochar

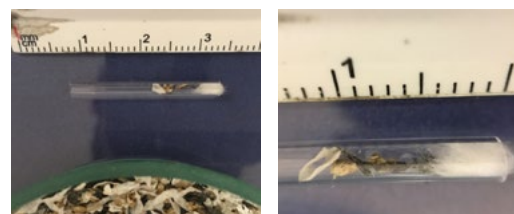


7. PCA plot for different biochars

8. PCA plot for different biochars contaminated by the various amount of external fuels

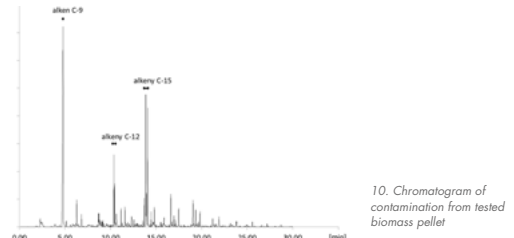
Combined the Py-GC-MS as an analytical method with PCA as an exploration data method, it is possible to determine what kind of biomass was applied to pyrolysis process and determine what it was contaminated with and in what amount.

Plastics residue analysis in biomass pellets



9. The separated fraction of contaminants from the tested biomass pellet sample

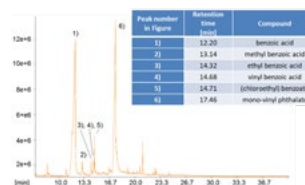
In this application, a 5 mg sample of ash was placed in a quartz tube reactor, inserted into the pyrolysis module. The sample was heated to 700°C at a rate of 5°C/sec and kept at that temperature for 10 min. All vapours were transferred to the CIS-4 (Gerstel) and held at -150°C (cooled with liquid nitrogen).



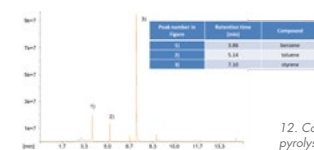
10. Chromatogram of contamination from tested biomass pellet

The analysis of Py-GC-MS confirmed the preliminary observation that the commercially available biomass pellets contained some polymeric parts. According to Polish law, such material no longer constitutes fuel and cannot be offered and sold on the market.

Detection of illegal waste combustion in domestic boilers

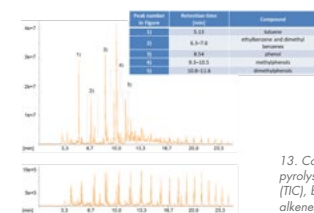


11. Combustion of PET with coal: analytical pyrolysis of an ash sample [1].



12. Combustion of PS with coal: analytical pyrolysis of an ash sample [1].

In this application, the same pyrolysis process conditions as described above for plastics residue analysis in biomass pellets were applied



13. Combustion of LDPE with coal: analytical pyrolysis of an ash sample. a) total ion current (TIC), b) ions characteristic of alkenes and alkenes: 55, 57, 69 and 71 Da [1]

In this approach, we presented an analytical technique for determining illegal waste combustion in heating devices. This method can detect the combustion of plastic wastes and provides some information about the type of plastic that was burned.

Conclusions

Our study presented several analytical approaches for determining the origin of contamination in the solid biofuels such as biomass pellets and biochars and illegal waste combustion in heating devices. This method is based on analytical pyrolysis and requires a GC coupled with an analytical pyrolyser. This method can detect the combustion of plastic wastes and provide some information about the type of plastic burned.

Utilising multivariate chemometric analysis in this application could develop a quantitative regression model to predict biochar polluted level. While our studies were identified, markers (chemical components) indicate the specific pollution of external fossil fuels. Except for this one, the Py-GC-MS analysis combined with Principal Component analysis is also very useful to determine the test biochar type.

Acknowledgements

This research was conducted in the Institute for Chemical Processing of Coal in Poland and funded by the Ministry of Science and Higher Education under the Iuventus Plus Program (project No. IP2014 041073) and Statutory R&D Project IChPW no. 11.17.003 and 11.19.001.

[1] Muzyka, R., Chrubasik, M., Pogoda, M. et al. Py-GC-MS and PCA Analysis Approach for the Detection of Illegal Waste Combustion Processes In Central Heating Furnaces. *Chromatographia* 82, 1101–1109 (2019). <https://doi.org/10.1007/s10337-019-03747-4>

INVESTIGATION OF BAIJIU AROMA TYPES AND REGIONAL ORIGIN

BY GC×GC-TOFMS IN CONVENTIONAL AND REVERSED COLUMN CONFIGURATION

Xi He | Faculty of Food Science and Nutrition / Poznań University of Life Sciences, Wojska Polskiego 31, 60-624 Poznań, Poland

Henryk. H. Jeleń | Faculty of Food Science and Nutrition / Poznań University of Life Sciences, Wojska Polskiego 31, 60-624 Poznań, Poland

Introduction

The manufacturing process of Baijiu is very complex compared to other strong alcohols with the mixed microbial cultures, unique saccharification and spontaneous fermentation and lack of rectification. It imparts the liquor with its distinctive aroma and further enhances the richness and complexity of volatile compounds. The routine one-dimensional gas chromatography is incapable of separating the complex volatiles of Baijiu satisfactorily. Therefore, comprehensive two-dimensional gas chromatography is suggested for resolving polar compounds present in alcoholic beverages, the reversed column setup application was tested in our study. The conventional column setup as a traditional configuration was also included in the investigation. The orthogonality, aroma types classification and regional origin classification were explored.

Materials and methods

Baijiu samples (65) were purchased from Chinese liquor stores. The information regarding the aroma types and regional origin included in our study was displayed in **Figure 1**. The main analytical strategies and results comparison approaches were demonstrated in **Figure 2**.

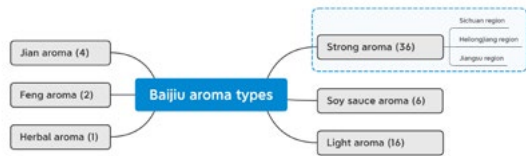


Figure 1. Baijiu samples information involved in the study

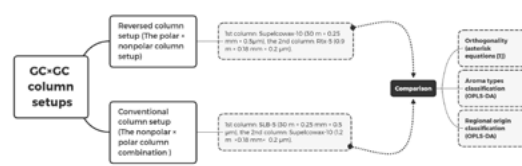


Figure 2. The main analytical methods and strategies

Results

Orthogonality comparison

To completely use the potential of multi-dimensional chromatography to achieve the maximum separation power possible, it is essential that the separation mechanisms used in each dimension be independent of each other – the two dimensions should be orthogonal.

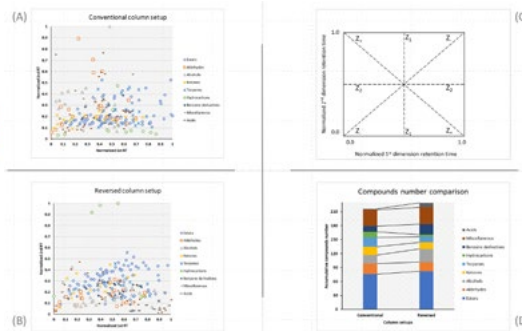


Figure 3. (A) GC×GC separations of Baijiu samples from conventional column setup, (B) GC×GC separations of Baijiu samples from reversed column setup, (C) Graphical illustration of parameters from asterisk equation [1], (D) Compounds number comparison between different chemical groups from conventional (216 compounds in total) and reversed column setup (229 compounds in total).

The orthogonality measuring method was adopted from the paper of Camenzuli and Schoenmakers [1], in which they introduced a set of asterisk equations enable to not only measure the orthogonality but also provide facilitated comparison of different multi-dimensional methods between systems and samples by providing more information about the location of the peaks within the separation space (**Figure 3**, (C)). Our study with the analysis of Baijiu samples the reversed column setup ($A_0=45.13\%$) presents a better separation power than the conventional one ($A_0=43.92\%$).

Classification of aroma type

Considering the great variety present in our Baijiu samples, a strategy for lowering the 'noise' presented in the dataset was adopted by integrating the orthogonal signal correction (OSC) filter. Orthogonal partial least squares discriminant analysis (OPLS-DA) is applied to discriminate 6 Baijiu aroma groups. Models from the conventional and reversed setups both presented an excellent predictive power in the classification of the Soy sauce, Light, Herbal and Feng aromas, however, regarding Jian and Strong aroma, the model based on the conventional setup showed better discriminative performance (**Figure 4**), which was confirmed by both internal and external validation.

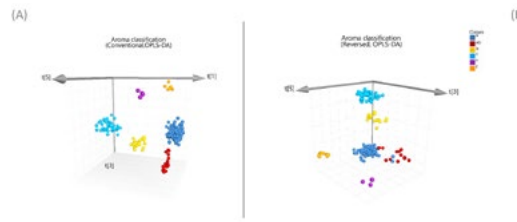


Figure 4. a: Strong aroma, ab: Jian aroma, b: Soy sauce aroma, c: Light aroma, x: Herbal aroma, f: Feng aroma, OPLS-DA model based on conventional setup (A): $R^2Y=0.875$, $Q^2=0.861$; OPLS-DA model based on reversed setup (B): $R^2Y=0.851$, $Q^2=0.827$. R^2Y : Total explained fraction of the variation of Y block (aroma types), Q^2 : Total fraction of the variation of Y block (aroma types) that can be predicted.

Classification of regional origin

For the regional classification, both models based on conventional and reversed setups presented perfect model fitness and predictive ability to classify the Strong aroma Baijiu originating from the Sichuan, Heilongjiang, and Jiangsu regions (**Figure 5**). Besides, two validation methods were applied in our study and all the predictive abilities evaluated by the internal validation were further confirmed by the external validation.

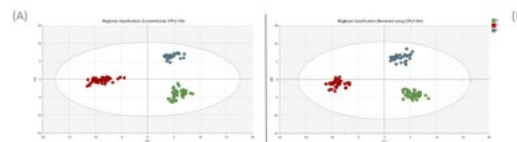


Figure 5. A: Sichuan, C: Heilongjiang, S: Jiangsu, OPLS-DA model based on conventional setup (A): $R^2Y=0.961$, $Q^2=0.951$; OPLS-DA model based on reversed setup (B): $R^2Y=0.961$, $Q^2=0.941$. R^2Y : Total explained fraction of the variation of Y block (regional origins), Q^2 : Total fraction of the variation of Y block (regional origins) that can be predicted.

Conclusion

A better classification for the Strong and Jian aroma types of Baijiu was achieved by the model built from conventional column setup. For the regional classification, both models from conventional and reversed setups showed perfect model fitness and predictive ability to classify the Strong aroma Baijiu originating from the Sichuan, Heilongjiang, and Jiangsu regions.

Comparing these results with our previous works on the same subject using one-dimensional gas chromatography with simultaneous injection into two columns [2] and classification performed using quasi electronic noses (SPME-MS, fast GC-based E-nose)[3], SPME-GC×GC-TOFMS showed the benefits of using high number of peaks obtained by GC×GC for subsequent statistical analysis: Approach [2] enabled quantification of 62 compounds, however, data obtained allowed for only partial separation of different aromas and it was not possible to separate the Baijiu from different regions. Approach [3] using the same classifier (OPLS-DA), indicated that the aroma classification models built from SPME-MS and GC based E-nose both met difficulties in the separation among Strong, Jian and Feng aroma groups. This problem was greatly improved by applying GC×GC-TOFMS configuring conventional column setup. The regional classification model based on SPME-MS achieved a complete classification with total correct classification rate 100%, as same as in this investigation. Still, referring to the fast GC based E-nose, the misclassification occurred among Sichuan, Heilongjiang and Jiangsu regions, the model achieved a total correct regional classification rate was 93.94% [3].

To summarize, of all investigated approaches, SPME-GC×GC-TOFMS proved to be of highest potential for aroma and regional classification of Baijiu.

FOOTNOTES: The content of this poster has been published: X. He, H.H. Jeleń, Comprehensive two-dimensional gas chromatography–time of flight mass spectrometry (GC×GC-TOFMS) in conventional and reversed column configuration for the investigation of Baijiu aroma types and regional origin, Journal of Chromatography A. 1636 (2021) 461774. <https://doi.org/10.1016/j.chroma.2020.461774>

[1] M. Camenzuli, P.J. Schoenmakers, A new measure of orthogonality for multi-dimensional chromatography, Anal. Chim. Acta. 838 (2014) 93–101. <https://doi.org/10.1016/j.aca.2014.05.048>.

[2] X. He, A. Gaca, H.H. Jeleń, Determination of volatile compounds in Baijiu using simultaneous chromatographic analysis on two columns, Journal of the Institute of Brewing. 126 (2020) 206–212. <https://doi.org/10.1002/jib.603>

[3] X. He, H. Yangming, E. Górska-Horczyk, A. Wierzbicka, H.H. Jeleń, Rapid analysis of Baijiu volatile compounds fingerprint for their aroma and regional origin authenticity assessment, Food Chem. 337 (2021). <https://doi.org/10.1016/j.foodchem.2020.128002>.

PYRO-GC×GC-TOFMS/FID FOR THE STUDY OF ORGANIC MATTER IN UNCONVENTIONAL HYDROCARBON RESERVOIRS

E. Leushina | Skoltech | Moscow, Russia
 E. Kozlova | Skoltech | Moscow, Russia
 T. Bulatov | Skoltech | Moscow, Russia
 M. Spasennykh | Skoltech | Moscow, Russia

Introduction

The work is devoted to analysis of organic matter in core samples from source rock formation. The objective is to evaluate hydrocarbon generation potential of the rocks based on current organic matter content and composition and reconstruction of sedimentation conditions that controlled organic matter accumulation.

Source rocks contain different forms of organic matter: gas and liquid hydrocarbons, heavy compounds and insoluble organic matter-kerogen. Content of each component may vary depending on formation and type of the rock. In this study, we applied Rock-Eval pyrolysis for bulk geochemical characterization of rocks and Pyro-GC×GC-TOFMS/FID at 350°C and 500°C for detailed analysis of organic matter composition [1]–[4]. To evaluate genesis of the organic matter and paleo-redox environment during marine sedimentation process we applied biomarker analysis of thermal extracts. The data were integrated to estimate organic matter genesis and perform productivity assessment.

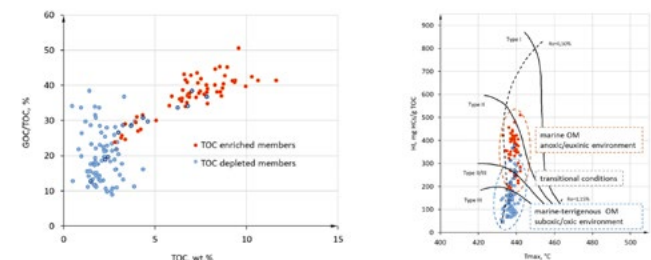
Geological object

The object of the study is unconventional hydrocarbon reservoir (shale) with layered structure: there are TOC enriched and depleted intervals within the cross-section. Based on TOC and U content, in total 19 m of the core we distinguished 7 lithological members with thickness varying from 1 to 3.7 m and 5.9 m of underlying deposits.

Instruments and methods

TOC measurements and Rock-Eval pyrolysis were performed using HAWK RW (Wildcat Technologies); U content measurements – elemental gamma logger (Coretest Systems); Pyro-GC×GC-TOFMS/FID – Pegasus 4D (LECO) with thermal desorption and pyrolysis injection units (Gerstel).

We used TOC and U content for 150 samples (19 m of core) in combination with biomarker analysis of thermal extracts for one sample per member to characterize the quantity and quality of organic matter and estimate paleo sedimentation conditions.



1. Rock-Eval pyrolysis data for the studied cross-section: total organic carbon content (TOC), pyrolyzable organic carbon vs TOC (GOC/TOC), temperature of maximum hydrocarbon generation (Tmax), total hydrocarbons derived from TOC (H)

Results and discussion

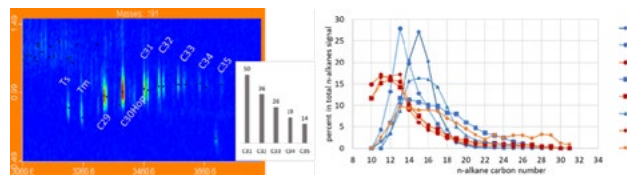
Benchmark of 5 wt.% TOC was set to discriminate members in the cross-section (Fig.2). Thus, there are four members, that are TOC depleted (<5 wt.%), and there are four TOC enriched members (>5 wt.%). Organic matter maturity level is at the beginning of the oil window for the studied rocks.

Member	Thickness, m	Lithology	TOC average, wt %	U average, ppm	Main product of kerogen decomposition
#8	3.7	Siliceous claystone with pyrite, bioturbated	2.0	2.7	Gas
#7	1.4	Kerogen containing siliceous claystone	7.6	19.1	Oil
#6	1.0	Siliceous claystone with pyrite, bioturbated	1.9	1.8	Gas and condensate
#5	1.2	Kerogen containing siliceous claystone with pyrite	7.1	20.6	Oil
#4	1.5	Kerogen containing siliceous claystone with pyrite	4.3	12.5	Gas and condensate
#3	1.2	Kerogen containing siliceous laminated claystone	8.8	25.6	Oil
#2	2.6	Kerogen containing carbonate-siliceous claystone	5.5	4.8	Oil
#1	5.9	Siliceous silty claystone	2.2	1.1	Gas

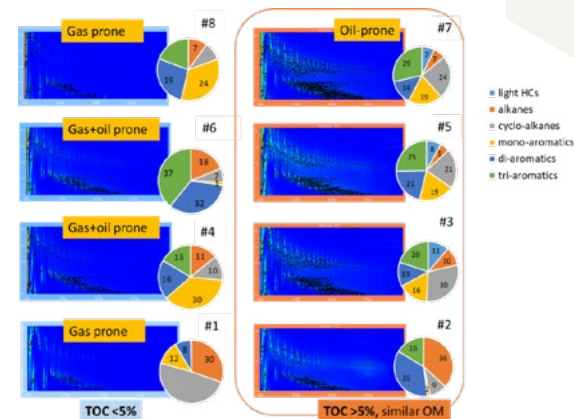
2. Cross-section averaged characteristics. 8 members are distinguished

For TOC enriched members #2, #3, #5, #7, we have found elevated U concentration and oil-prone kerogen in rocks (Fig.4), which was formed in anoxic/euxinic conditions from buried marine organic matter. On modified van Krevelen diagram (Fig. 1), these intervals correspond to organic matter type II (orange-red markers).

We have found little differences in composition of thermal extracts from samples #2, #3, #5, #7. The main features are similar: n-alkanes and hopanes fingerprint, C29/C30Hop <1, predominance of C27 regular steranes over C28 and C29 [4], and correspond to source rocks containing marine organic matter.



3. Composition of rock thermal extracts at 350°C: hopanes distribution for samples from TOC enriched members #1-2, 3, 5, 7 (left) and n-alkanes distribution (right)



4. Petroleum generation potential: composition of kerogen decomposition products at 500°C

TOC depleted members show variations in composition of organic matter and U content (blue markers on Fig.1). Organic matter in core samples from intervals #1, #6 and #8 has mixed origin with noticeable terrigenous input and accumulated under oxic environment (low U, organic matter type III). The rocks show moderate gas generation potential (Fig.4). For member #4, we estimated transitional accumulation conditions: moderate terrigenous influx and anoxic/suboxic conditions (moderate U, mixed organic matter type II-III). The resulting rocks demonstrate the potential to generate gas and gas condensate (Fig.3).

In contrast to biomarker composition of thermal extracts from TOC enriched rocks, intervals #4, 6, 8 contain only trace amounts of homohopanes C31-C35 and show elevated C29/C30 Hop ratio, which is additional evidence for terrigenous OM input resulted from river water inflow. Extract from #1 contains no hopanes, which is an indicator of lacustrine oxic conditions during sedimentation [4].

Conclusion

We have studied organic matter in core samples of source rocks (in form of petroleum and kerogen) using thermal desorption and pyrolysis unit coupled to GC×GC-TOFMS/FID. We applied this method for analysis of molecular composition of organic matter and its transformation products. The obtained data were integrated with the results of Rock-Eval pyrolysis, U content measurements, and geological information. For different intervals of the studied cross-section, we have evaluated sources of initial organic matter, sedimentation and maturation conditions.

As a result, we reconstructed the genesis of the source rock formation, identified potentially gas- and oil-prone intervals, and evaluated the productivity of the deposits.

References

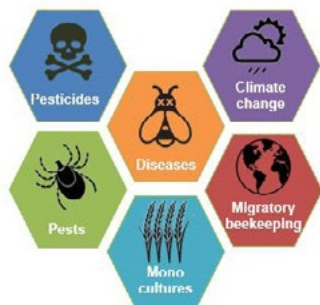
- [1] J. Espitalie and M. Bordenave, "Rock-Eval pyrolysis," *Appl. Pet. Geochemistry*, pp. 237–361, 1993.
- [2] P. B. Hall, D. Stoddart, M. Bjorøy, S. R. Larter, and J. E. Brasher, "Detection of petroleum heterogeneity in Eldfisk and satellite fields using thermal extraction, pyrolysis-GC, GC-MS and isotope techniques," *Org. Geochem.*, vol. 22, no. 3–5, pp. 383–402, 1994.
- [3] M. Bjorøy, K. Hall, and P. B. Hall, "Detailed hydrocarbon analyser for well site and laboratory use," *Mar. Pet. Geol.*, vol. 9, pp. 648–665, 1992.
- [4] K. E. Peters, C. C. Walters, and J. M. Moldovan, *The Biomarker Guide: Volume 2, Biomarkers and Isotopes in Petroleum exploration and Earth History*. Cambridge: Cambridge University Press, 2005.

DETECTION OF HONEY BEE DISEASE THROUGH MONITORING SHIFTS IN VOLATILE PROFILES

Margaret Gill | Keele University / Newcastle Under Lyme, Staffordshire, ST5 5BG, UK. Correspondences to m.c.gill@keele.ac.uk
Falko Drijfhout | Keele University / Newcastle Under Lyme, Staffordshire, ST5 5BG, UK.

Introduction

Significant declines in honeybee numbers have been reported globally, which cost the economy an estimated \$15 billion a year. Honeybees face many disease and pest pressures, and early detection and treatment significantly improves honeybee colony survival. The analysis of volatile organic compounds is used for the early detection of human diseases. The aim of this research is to identify VOCs associated with honeybee diseases and pests using head space analysis and GCxGC-TOF MS to develop sensors for earlier disease detection which could facilitate more efficient treatment and control methods.



Honey bee diseases and pests

The term colony collapse disorder (CCD) was coined in the United States to describe unexplained large-scale ongoing losses of honey bee colonies. The declining trend in honey bee numbers and CCD have yet to be attributed to any one cause, but multiple factors such as pesticide use, agricultural and bee keeping practices and climate change have been shown to contribute. Honey bees face numerous disease and pest pressures, and the early detection and treatment of diseases and pests have been shown to significantly improve honey bee colony survival. Details of some of the more significant diseases and pests are outlined below.

American foulbrood (AFB) – Paenibacillus larvae

A rod-shaped spore forming gram positive bacteria. Larvae become infected when fed brood food containing spores. The infection kills the larvae at the pro-pupal stage of development and symptoms include wax capping's which are greasy, sunken and dark with perforations, and the formation of a mucus rope when the cell contents is agitated with a small stick and withdrawn. Destruction of infected colonies is currently the only effective method of eradication, and due to this P. larvae is a notifiable disease in most countries worldwide.

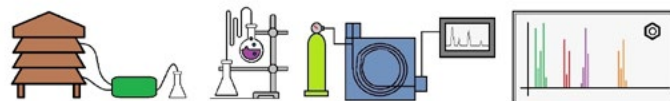
European foulbrood (EFB) – Melissococcus plutonius

A gram-negative lance shaped bacteria. Larvae become infected when fed brood food containing the bacteria, where the bacteria multiply in the larval gut and competes with the larvae for food. The infection does not always kill the infected larvae if there is sufficient food to feed both, and symptoms include melted looking discoloured larvae which lie in the cells in unnatural positions. EFB infections are problematic to resolve as antibiotic treatments contaminate hive products and biotechnological methods are time consuming and complicated to complete.

Varroa – Varroa destructor

A parasitic mite of honey bees which reproduce in comb cells and feed on the honey bee pupae, weakening the pupae and the colony as a whole. Mites feeding on pupae also increase transmission of viruses such as deformed wing virus (DWV). Treatment of infested colonies is problematic as mites can develop resistance to some chemical treatments, which can also contaminate hive products. Other methods of control are either costly, time consuming or complex making varroa a significant threat to honey bee populations.

There are also numerous minor diseases and pests which affect colonies of honey bees, and whilst singularly they may not be detrimental to the colony, in combination with other diseases, pests and environmental pressures they contribute significantly to honey bee declines.



Volatile collection and analysis

A variety of sampling techniques, such as head space analysis and dynamic flow systems using both MonoTrap™ and Pye entrainment with tenax tubes will be used in laboratory conditions to collect VOCs from isolated samples of diseases, pests, bees, equipment and hive products. The same equipment and techniques will be used to collect VOCs from healthy and infected honey bee colonies in the field.

Volatile profiles of all samples will be obtained on a PEGASUS® BT GC-TOFMS. Splitless injection is typically used in honey bee VOC research as the proportion of analytes of interest in the sample is generally small (<0.01%), and splitless injection maximises the amount of analytes that will reach the column. To help prevent the thermal degradation of unstable compounds from the extremely high temperatures used in the injector ports, cool-on-column injector ports can be used. A DB-35 column is suitable for the analysis of honey bee VOC which tend to be comprised of polar compounds.

TOFMS has a very high mass resolving power which allows for a retrospective look at potential small molecule analytes that may be present in samples and is useful when screening for unknown analyte which is useful for honey bee VOC research.

Multivariate statistical analysis of peak / ion pairs will be used to identify volatile profile which will allow for the identification of disease and pest biomarkers.

Sampling undertaken over multiple seasons to monitor shifts in the natural variations of the volatile profiles of healthy and diseased colonies which will enable the development of field based diagnostic tools for early detection of honey bee diseases and pests.



PEGASUS® BT GC-TOFMS

GREEN AND SUSTAINABLE CATALYSIS USING A PALLADIUM DOPED BIOCHAR UNDER MILD CONDITIONS

Jamie P. Southouse¹, Karl Hornsby^{1,2}, Kin Wai Cheah^{1,2}, M. Grazia Francesconi³, Vasiliki Skoulou^{1,2} and Martin J. Taylor^{1,2*}

¹ Energy and Environment Institute, University of Hull, Cottingham Road, Hull, HU6 7RX, United Kingdom

² B³ Challenge Group, Department of Chemical Engineering, University of Hull, Cottingham Road, Hull, HU6 7RX, United Kingdom

³ Department of Chemistry, University of Hull, Cottingham Road, Hull, HU6 7RX, United Kingdom

* Corresponding author: Martin.Taylor@Hull.ac.uk

Abstract

With ever increasing scrutiny of how industrial chemistry is conducted, biochar offers a route to the preparation of green heterogeneous catalysts. Biochar is simply prepared by the pyrolysis of pretreated lignocellulosic biomass in an inert atmosphere. Biochar supported Pd nanoparticles showed great potential in the liquid phase selective hydrogenation of phenylacetylene under mild conditions, without sacrificing activity, as validated by the LECO GCxGC 7890B. It was found that varying the pyrolysis temperature altered the activity of the Pd/Char catalyst resulting in an activation energy as low as 10 kJ mol⁻¹.

Introduction

To lower energy requirements and provide greener, more sustainable options for the production of fine chemicals and fuels, the use of catalysts derived from waste materials has gained attention. Specifically, the use of carbonised lignocellulosic biomass as a support material.¹ The biochar support is produced via the slow pyrolysis of biomass in an inert atmosphere and can then be doped with a metal generating a functionalised biochar derived catalyst. These have seen significant interest as compared to other commercial catalysts like metal oxides as biomass is cheap, requiring no ore extraction/refinement with readily available renewable stocks.² The lignocellulosic waste used in this work is barley straw, a highly abundant feedstock. Before use, these waste streams must undergo pre-treatments (milling, leaching) to remove the presence of any additional metal such as alkali and alkali earth metals (AAEM). AAEM are known to degrade the char during the pyrolysis process, thereby reducing the biochar yield. Whilst the presence of AAEM complicates biochar production it is negligible compared to the shortcomings of current industrial methods.

Styrene is a key industrial compound used in the synthesis of polymers vital for the modern world, such as ABS, EPS and PS. The global demand for styrene has increased by 500% since 1983. Industrially styrene is produced through the energy intense dehydrogenation of ethylbenzene using potassium iron (III) oxide as a catalyst at 600-650 °C, accounting for 99% of global ethylbenzene demand in 2020 so far. Due to this energy intensive process the production of styrene has a massive environmental strain. As such new methods look to produce styrene from the selective hydrogenation of phenylacetylene under very mild conditions with high selectivity.³

Our goal is to expand on this process using, biochar supported catalysts to sustainably produce styrene from phenylacetylene under mild conditions, achieving high selectivity and high conversion of the phenylacetylene in the liquid phase. This would be tested using palladium supported on biochars pyrolyzed at a range of temperatures to determine if there are physical or chemical alterations to the support that can promote the phenylacetylene hydrogenation.

Biochar preparation
Barley straw, a highly abundant herbaceous and low-quality feedstock was milled (10,000 RPM) using a Retsch GM200 Knife Mill for 1 min, followed by separating via a Retsch AM200 sieve stock to reclaim <250 μm particles. These fractions were then pretreated via leaching in deionized water, with a feedstock ratio of 10 g L⁻¹ for 24 h at 25 °C. The slurry was separated and dried under vacuo before drying in a Fisherbrand Gravity Convection Oven at 105 °C for 24 h, according to ASTM standards.⁴ The leached feedstock was pyrolysed in a tube furnace at 500 °C, 600 °C or 700 °C (5 °C/min heating rate, holding for 1 h) under N₂ flow. This was left to cool to room temperature under a N₂ flow to prevent the char combusting. Biochar was then washed with 20 mL deionised water, ethanol and acetone before subsequently dried at 105 °C for 24 h.

References

- Sadjadi, S.; Akbari, M.; B., L.; Monflier, E.; Heravi, M. M., Eggplant-Derived Biochar-Halloysite Nanocomposite as Supports of Pd Nanoparticles for the Catalytic Hydrogenation of Nitroarenes in the Presence of Cyclodextrin. *ACS Sustain. Chem. Eng.* **2019**, *7* (7), 6720-6731.
- Wang, Y.; Ling, L.; Jiang, H., Selective hydrogenation of lignin to produce chemical commodities by using a biochar supported Ni-Mo₂C catalyst obtained from biomass. *Green Chem.* **2016**, *18*, 4032-4041.
- Dominguez-Dominguez, S.; Berenguer-Murcia, A.; Linares-Solano, A.; Carzola-Amaros, D., Inorganic materials as supports for palladium nanoparticles: Application in the semi-hydrogenation of phenylacetylene. *J. Catal.* **2008**, *257* (1), 87-95.
- Alabdralameer, H. A.; Taylor, M. J.; Kauppinen, J.; Saini, T.; Pitkäräinen, T.; Skoulou, V., Big problem, little answer: overcoming bed agglomeration and reactor slugging during the gasification of barley straw under continuous operation. *Sustain. Energy Fuels* **2020**.
- Cheah, K. W.; Taylor, M. J.; Osaishitani, A.; Beaumont, S. K.; Nowakowski, D. J.; Yusup, S.; Bridgewater, A. V.; Kyriakou, G., Monometallic and bimetallic catalysts based on Pd, Cu and Ni for hydrogen transfer deoxygenation of a prototypical fatty acid to diesel range hydrocarbons. *Catal. Today* **2019**, *324*, 115-125.

Catalyst preparation

A series of biochar supported Pd catalysts were prepared via incipient wetness impregnation (IW).⁵ The nominal metal loading of all catalysts synthesised was kept constant at 5 wt. %. Three types of monometallic catalysts Pd/C₅₀₀, Pd/C₆₀₀ and Pd/C₇₀₀ were prepared. In a typical synthesis of Pd/Biochar, biochar was impregnated with the appropriate amount of Pd(ac), (Sigma Aldrich). Before adding the saturated solutions of corresponding metal salts to the bare support, the solutions were sonicated in a water bath for 0.5 h to ensure complete metal salt dissolution. After sonication, the solutions were dispersed onto the support under continuous stirring at room temperature for 2 h before heating to 80 °C and aging overnight. Subsequently, the catalyst slurries were collected, annealed and reduced under flowing 10% H₂/N₂ at 450 °C for 2 h at 5 °C/min.

Biochar and Catalyst Characterisation

Scanning Electron Microscopy (SEM) images were acquired via a Zeiss EVO 60 instrument at a pressure of 10⁻² Pa and an electron acceleration potential of 20 kV (Figure 2). Energy Dispersed X-ray spectroscopy (EDX) was carried out on bare biochars using an Oxford Instruments Inca System 350 (Table 1). Fourier Transform Infrared (FTIR) spectra were obtained using a Thermo Scientific Nicolet iS5 instrument fitted with a PIKE MIRAcle single reflection horizontal ATR accessory (Figure 3). Powder X-Ray Diffraction (PXRD) patterns were acquired using a Malvern Panalytical Empyrean diffractometer (Figure 4).

Catalyst testing

Catalytic testing of 5 wt% palladium supported on waste derived biochars was carried out using a parallel batch reactor set up using a Radleys Carousel Reaction Station. Mixtures of phenylacetylene (0.25 M), ethanol (25 mL) and toluene (0.2 M) as an internal standard were charged to the reactor along with 50 mg Pd/Char. Hydrogen gas (99.99%) was bubbled through the stirred reaction mixture and mixed at 600 rpm across various temperatures. Aliquots of the reaction solutions were removed periodically, filtered, diluted and analysed offline on a LECO GCxGC7890B (Figure 1 and Figure 5).

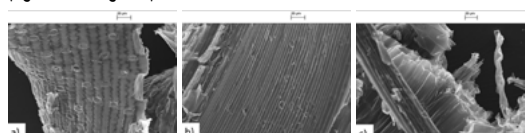


Figure 2: SEM images of biochars produced by slow pyrolysis at a) 500 °C, b) 600 °C and c) 700 °C

Results

Catalyst Characterisation

Figure 2a-c shows SEM images for slow pyrolyzed biochars prepared at 500 °C, 600 °C and 700 °C, respectively. All images show the effect of pyrolysis temperature on the resultant biochar morphology and structure. The surface morphology of the char materials show increasing disruption to the biomass surface with increasing pyrolysis temperature. Figure 2a, clearly shows the stomata remaining undisturbed by the pyrolysis process, showing the limited impact the process has on the physical structure in the resultant biochar. Yet, when the temperature is increased to 600 °C (Figure 2b), the stomata structures show disruption from their original morphology, in addition to the early signs of delamination of the structure resulting in fraying of the particle edges. At 700 °C (Figure 2c) the resultant biochar structure has been greatly disrupted with no stomata visible and clear delamination of the lignocellulosic structure.

EDX analysis of the biochar materials showed successful pyrolysis of the biomass, with the predominant element within all samples being carbon (>83 wt%). These results are summarised in Table 1. Of interest was the decrease in oxygen content between biochars prepared at 500 °C and those

prepared at higher temperatures, with an approximately 6 wt% difference in oxygen content between these samples. This discrepancy in oxygen content was determined to be due to the release of aromatic alcohols from within the lignin structure at higher pyrolysis temperatures. Trace amounts of other elements were expected to be present in the biochar materials, with these elements being non-water soluble, their removal from the waste material is problematic. However, none are expected to show catalytic properties, nor will they promote hydrogen based catalytic transformations.

Element	wt%		
	500 °C	600 °C	700 °C
C	83.43	89.32	85.76
O	13.46	7.67	7.34
F	0	1.61	1.19
Mg	0	0	0.25
Si	0.92	0.27	0.44
K	0.84	0	0.85
Ca	1.35	1.13	4.16

Table 1: Summary of EDX analysis of biochars analysed at different temperatures

FTIR was carried out on all biochars before impregnation (Figures 3a, 3c and 3e) and after with Pd (Figures 3b, 3d and 3f). The impregnation followed by annealing and reduction was determined not to influence the chemical nature of the biochar. This is shown by the lack of additional visible peaks, corresponding to acetate in the Pd impregnated samples.

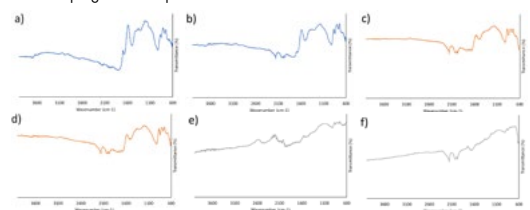


Figure 3: FTIR of bare biochars and Pd impregnated chars, a) 500 °C, b) 5% Pd/500 °C, c) 600 °C, d) 5% Pd/600 °C, e) 700 °C and f) 5% Pd/700 °C

PXRD was carried out on the biochars before and after Pd impregnation to determine the presence of any crystalline phases within the biochar and to determine the presence of Pd within the impregnated biochars. For the bare biochars, there was no distinct crystalline graphite phase at any temperature indicating that the carbon present was amorphous in nature (Figure 4a), where the blue line is the carbon at 500 °C, yellow is 600 °C and grey is 700 °C. Once impregnated with Pd, annealed and reduced, clear peaks attributed to cubic Pd (Fm3 m) can be identified (Figure 4b) showing the presence of Pd(0) in the sample. The absence of peaks attributable to palladium oxide or palladium acetate, shows the successful decomposition of the Pd precursor and reduction of Pd(II) to Pd(0).

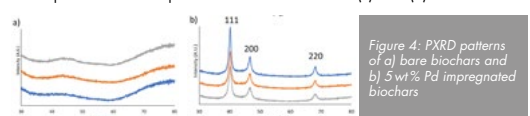


Figure 4: PXRD patterns of a) bare biochars and b) 5 wt% Pd impregnated biochars

Catalytic Testing

Selective hydrogenation of phenylacetylene (PA, blue line) to styrene (Sty, grey line), avoiding over conversion to ethylene benzene (EB, orange line), was carried out to probe the differences in catalytic activity of 5 wt% Pd/biochars pyrolyzed at different temperatures. The hydrogenation reactions were carried out at 25 °C,

40 °C and 70 °C, for all three catalysts (Figure 5). In all cases studied the greatest rate of PA conversion was seen with 5% Pd/700 °C catalyst. However, it was noted that 5% Pd/700 °C maintained selectivity of the Sty for longer than the other catalysts, only losing Sty selectivity once all PA had been consumed. The reactions carried out at using 500 °C biochar supported Pd, were dramatically slower than those carried out using the other two biochar supported catalysts. This may have been due to the higher oxygen content of the 500 °C biochar interfering with substrate binding. The 600 °C catalyst showed similar activity to that of the 700 °C catalyst, however, the Sty selectivity was lost more readily indicating a higher affinity of this catalyst for the reduction of Sty, inciting a greater overall activity not selectivity.

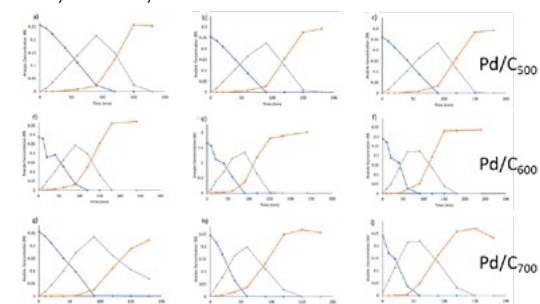


Figure 5: Reaction profiles for a) 5% Pd/500 °C at 25 °C, b) 5% Pd/500 °C at 40 °C, c) 5% Pd/500 °C at 70 °C, d) 5% Pd/600 °C at 25 °C, e) 5% Pd/600 °C at 40 °C, f) 5% Pd/600 °C at 70 °C, g) 5% Pd/700 °C at 25 °C, h) 5% Pd/700 °C at 40 °C and i) 5% Pd/700 °C at 70 °C

Activation energy of PA hydrogenation was calculated using Arrhenius modelling and the initial rate of PA consumption. The activation energy for the reaction was 10 kJ mol⁻¹, this low activation energy can be attributed to the high loading of Pd(0) and high loading of the catalyst within the reactor (~50 mg).

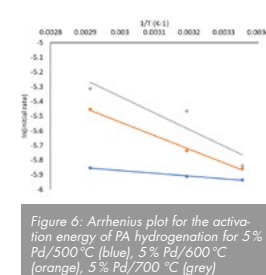


Figure 6: Arrhenius plot for the activation energy of PA hydrogenation for 5% Pd/500 °C (blue), 5% Pd/600 °C (orange), 5% Pd/700 °C (grey)

Conclusions

In the drive for more sustainable chemical processes a locally sourced biomass feedstock provides an avenue to provide a novel support option for the selective hydrogenation of phenylacetylene. By using scalable pre-treating and pyrolysis methods, biochars with different physical and chemical structures can be produced. These biochars can be impregnated with palladium via an easily scalable incipient wetness impregnation method. The resulting catalysts can be applied to the selective hydrogenation of phenylacetylene. In general it was observed that the higher the pyrolysis temperature of the support the more active the end catalyst proved to be, where by subtly altering the pyrolysis temperature the selectivity of the chemical reaction can be optimized.

Acknowledgements

All authors would like to greatly acknowledge the THYME project (UKRI, research England) for funding. We would like to especially thank Mr. Timothy Dunstan for the acquisition of SEM images.

We would like to sincerely thank all participants for their valuable contributions who made this competition a success. They encourage our aim of improving our understanding and knowledge of LECO users' work and research.

LECO Corporation

3000 Lakeview Avenue | St. Joseph, MI 49085
Phone: 269-985-5496
info@leco.com | www.leco.com

LECO Europe

eu.leco.com

